High-resolution morpho-tectonic profiling across an orogen

Necea, D.

2010

document version
Publisher's PDF, also known as Version of record

5 Cretaceous to Quaternary thermo-tectonic evolution revealed by low-T thermochronology

5.1. Introduction

Evolution of convergent mountain belts has been widely studied over the last decades. The amplitude and rate of orogenic evolution through time can be controlled and enhanced by the tectonic processes which tend to build up topography and by the surface processes which lower it. The distinction between processes acting and controlling shortening in the SE Carpathians is not simple and relies on constraining the amplitude and timing of vertical movements from the orogen itself and adjacent basins (Bertotti et al., 2003). Various methods can be applied to obtain constraints at different time scales. For the last orogenic phases, e.g. during the Quaternary, exposure age dating can be applied (Dunai, 2001; von Blanckenburg, 2006). In this study, no reference surfaces have been found for exposure age dating. Instead, geomorphology (Chapter 2) integrated with luminescence dating have been applied to loess deposits, documenting roughly 200-250 m of vertical movements (Chapter 4). To derive the older thermal and kinematic histories, low-T thermochronology (U-Th/He and AFT analyses) has been carried out for samples

Figure 5.1

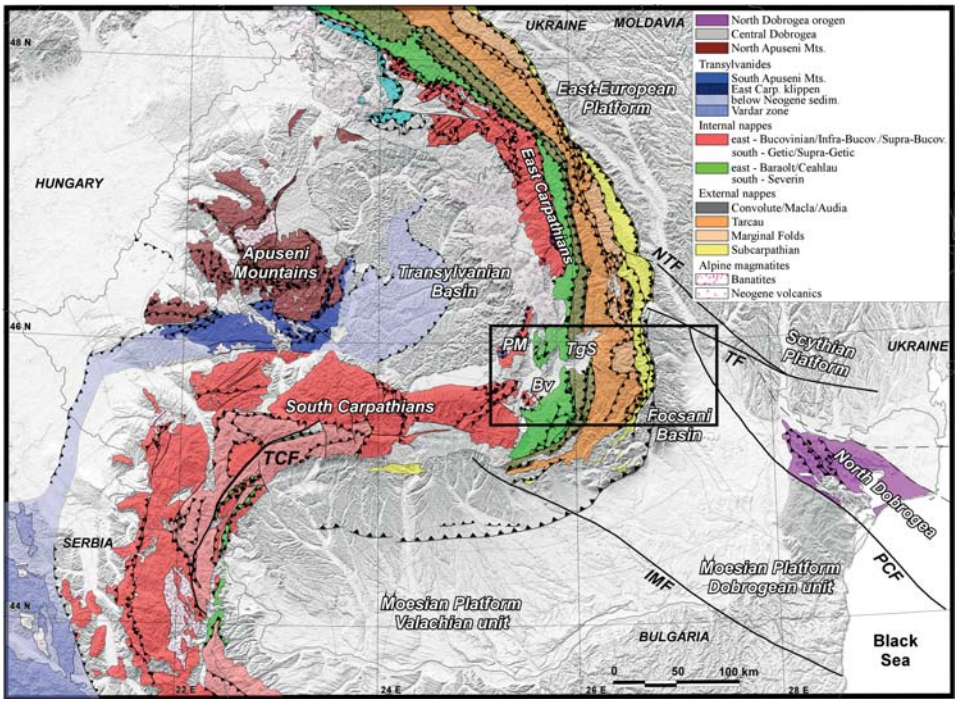

Regional geology of the Romanian Carpathians, where the black rectangle corresponds to the study area, the SE Carpathians bending zone. PM-Perşani mountains; Bv-Braşov and TgS-Târgu Secuiesc basins; NTF-New Trotuş fault, TF-Trotuş fault, IMF-Intramoesian fault and TCF-Timiş-Cerna fault (Matenco et al., 2007).

along a W-E oriented transect of 175 km (Fig. 5.2b). This starts in the Transylvanian basin, passes the internal metamorphic nappes and external thin-skinned wedge, and stops on the western tilted flank of the Focşani basin. Low-T thermochronology usually documents the cooling history experienced by rocks as they are exhumed in the 2-5 km of the upper crust (AFT and U-Th/He; Ehlers and Farley, 2003). A gap exists between the range of ages obtained from coupled geomorphology and luminescence dating and thermochronology. In this study, the late stage orogenic movements generating between 200 m and 2 km of uplift and erosion could not be quantified and therefore only average values could be estimated. Furthermore, provenance ages have been used to reconstruct the relationship between source and sink areas (Ruiz et al., 2004, 2005). Amplitude, timing and kinematics of shortening have been separately quantified, several tectonic phases being identified and related to the thermal and tectonic evolution of the SE Carpathians. This study incorporates results from the recent structural research in both geometry and evolution of the Transylvanian back-arc basin (Krézsek and Bally, 2006), Carpathians kinematics (Matenco et al., 2007; Leever et al., 2006), absolute age dating of basin sediments (Vasiliev et al., 2004; 2005) and orogen uplift (Sanders et al., 1999; Merten et al., 2005).

5.2. Tectonic units across the orogen and deformation time

5.2.1. Neotethys and Alpine Tethys oceanic spreading in the Carpathians

The oceanic spreading of the Tethys in the area of the Romanian Carpathians started during the Middle Triassic and continued until the Early Cretaceous, resulting in a first separation of two blocks to the west and to the east of the Tethys ocean, namely the Tizsa and Dacia units (Csontos and Vörös, 2004). The rifting time is given by the Middle Triassic-Jurassic oceanic deposits and ophiolites presently found in the deepest part of the Transylvanian basin, underneath the Neogene sediments, and also exposed at the surface in the Transylvanides klippen of the East Carpathians (i.e. Perşani Mountains; Săndulescu, 1988; Schmid et al., 2008; Hoeck and Ionescu, 2006; Fig. 5.1). Subsequent Late Jurassic intra-continental rifting affected to the east the “European domain”, leading to formation of the Ceahlău-Severin ocean, whose remnants are presently incorporated in the Baraolt/Ceahlău/Severin nappes (Fig. 5.1). Extension continued until the Early Cretaceous, when contraction and continental collision took place between the Tisza and Dacia blocks (intra-Albian; Săndulescu, 1988). Coeval, the Bucovinian nappes have been thrusted eastward over the more external Ceahlău-Severin units (Săndulescu, 1988).

5.2.2. Bucovinian/Getic nappe stack and Transylvanides

The Bucovinian nappe stack of the East Carpathians (Figs. 5.1 and 5.2; Popescu-Voiteşti, 1929) has the geometry of a large dome and consists of low to medium-grade metamorphic series of Late Precambrian-Cambrian age (Vodă, 1980). The intra-Albian E-vergent nappe stack truncates an earlier W-vergent nappe stack, supposedly of Variscan age, which exhumed higher-grade metamophic units to the east (Kräutner and Bindea, 2002). The uppermost unit is the Bucovinian nappe, which is composed of low- to medium-grade metamorphic series separated by pre-Alpine thrusts and of a Triassic to Lower Cretaceous sedimentary cover (Balintoni, 1981; Vodă, 1980). Upper Barremian-Albian wildflysch deposits with blocks in a turbiditic matrix are commonly interpreted as pre-

and syn- tectonic deposits underneath the overriding ophiolite-bearing Transylvanian nappes (Patrulius et al., 1969; Ştefănescu, 1976; Săndulescu, 1988). The Sub-Bucovinian nappe is composed of the same type of metamorphic basement as the Bucovinian nappe and has a Permian-Lower Cretaceous sedimentary cover with similar characteristics for the Mesozoic part. The lowermost Infra-Bucovinian nappe displays a medium-grade metamorphic basement and a Permian-Jurassic sedimentary cover, slightly metamorphosed in parts (Kräutner and Bindea, 2002). This unit crops out only in a few restricted tectonic windows in the core of the nappe stack. In the study area, outcrops of the Bucovinian nappe are observed mainly in the Perşani Mountains along the Olt river (Fig. 5.2).

The equivalents of these nappes in the South Carpathians are the Getic and Supragetic nappes (Fig. 5.1; Săndulescu, 1988), comprising a pre-Alpine basement with medium to high-grade metamorphic units and low-grade Paleozoic rocks, covered by an Upper Paleozoic to Lower Cretaceous sequence of conglomerates, quartzitic sandstones, shales and limestones.

The post-tectonic cover of the Bucovinian/Getic/Supragetic nappes starts with the Upper Albian-Cenomanian molasse-type deposits, indicating that the nappe stack has formed during the intra-Albian event ("Austrian" in Romanian literature). However, Upper Cretaceous rocks are locally also involved into the Latest Cretaceous ("Laramian") deformation (Săndulescu, 1988).

The intra-Albian contractional event is also responsible for the emplacement of the overlying Transylvanides nappes, which represent the remains of an oceanic domain that was part of the larger Neotethys area. It opened during the Late Triassic-Jurassic times ("the East Vardar ophiolites", Schmid et al., 2008). The typical outcropping area of these nappes are the South Apuseni Mountains (Fig. 5.1), but the ophiolites can be followed eastwards below the Neogene sediments of the Transylvanian basin and crop out as isolated klippen also on top of the East Carpathians. These klippen consist of Triassic to Albian sedimentary units, which have been equally deposited over the ophiolitic and continental units (Săndulescu, 1975; Hoeck and Ionescu, 2006), the eastern margin of this oceanic domain (Hoeck and Ionescu, 2006).

5.2.3. Ceahlău-Severin ocean

The ophiolite-bearing Ceahlău nappe (including the Black Flysch and Baraolt thrust sheets) is equivalent to the Severin nappe in the South Carpathians, together forming an accretionary wedge, which was docked to the overlying continental units (Bucovinian/Getic nappes) during the earlier described intra-Albian deformational event (Săndulescu, 1988). These two nappes represent the remnants of what is known as the Ceahlău-Severin ocean (Schmid et al., 2008).

The main body of this accretionary wedge is best exposed in the East Carpathians, where the Ceahlău nappe is the main unit. Here, the uppermost nappes are the Black Flysch and Baraolt nappes (Fig. 5.1). The Black Flysch nappe crops out only in the northern part of the Romanian Carpathians and exposes a basement made up of massive basaltic flows and dykes penetrating the overlying Kimmeridgian-Aptian sediments (Bleahu, 1962; Săndulescu, 1988). The equivalent of this unit near the southern termination of the East Carpathians is the Baraolt nappe (Ştefănescu, 1976), which is made up exclusively of Berriasian-Aptian sandy-calcareous turbidites. The lower and larger Ceahlău nappe is composed of several sedimentary sequences distributed in few thrust sheets. These sequences are: Upper Jurassic radiolarites with basic igneous rocks and deep water de-

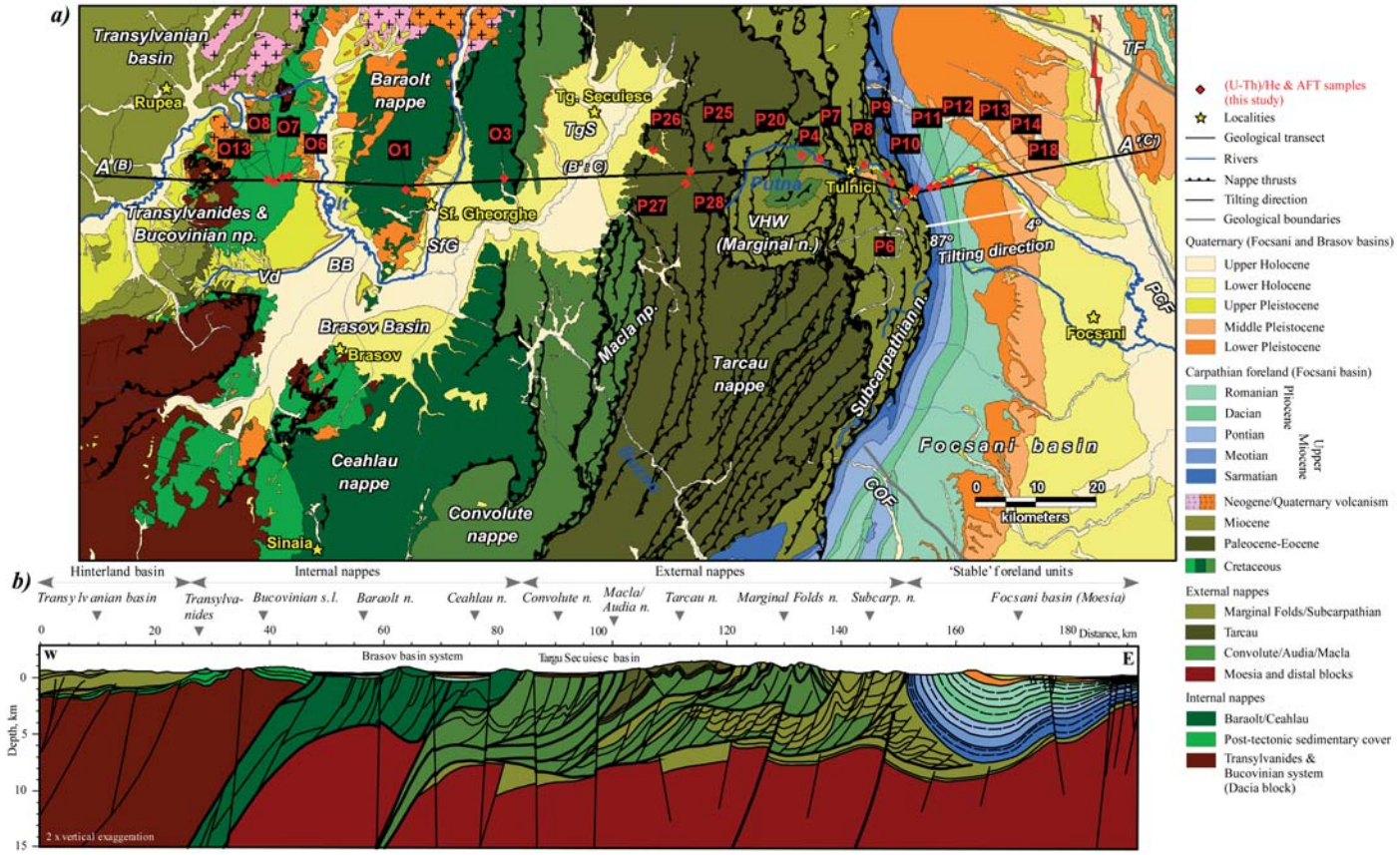

Figure 5.2

(a) Detailed geological map of the study area with sample locations collected along a W-E elevation transect of 175 km, the Olt-Putna profile (A-A'). Red rhombuses correspond to AFT and (U-Th)/He samples analyzed in this study. Vd-Vlădeni, BB-Bârsa-Baraolt, SfG-Sfântu Gheorghe sub-basins and TgS-Târgu Secuiesc basin; VHW-Vrancea half-window (Marginal Folds nappe); TF-Trotuş fault, IMF-Intramoesian fault and COF-Capidava-Ovidiu fault. (b) Geological cross-section along which sampling was performed starts in the Transylvanian hinterland and ends in the Focşani foreland basin (modified after Leever et al., 2006; Schmid et al., 2008).

posits (Azuga Formation), Tithonian-Neocomian mostly shaley and calcareous deposits (Sinaia Beds), Barremian-Aptian proximal turbidites (Comarnic Beds), Upper Aptian-Albian massive sandstones/conglomerates (Ceahlău and Bucegi Formations) and Vraconian-Cenomanian distal turbiditic formations (Patrulius, 1969; Ştefănescu, 1976).

The basement and overlying sediments of the Ceahlău-Severin ocean have been stacked during two events (Ştefănescu, 1976; Săndulescu, 1988). During the first event (Aptian-Albian; "Austrian phase"), all these units have been overthrust and attached to the overlying Getic/Bucovinian nappes. At the same time, the Baraolt and Black Flysch nappes have been emplaced over the more external Ceahlău nappe, as indicated by their Vraconian-Cenomanian post-tectonic cover (Săndulescu, 1988). The second deformational event took place during the Latest Cretaceous ("Laramian phase"), when the internal unit(s) came into present-day surface contact with the most external flysch units, such as the Convolute flysch nappe of the Miocene thrust belt in the East Carpathians, and with the Danubian nappe pile in the South Carpathians. The age of this event is constrained by the Upper Campanian-Maastrichtian post-tectonic cover ("red beds"; Săndulescu, 1988; Melinte and Jipa, 2005).

The Ceahlău-Severin nappe system is the only unit in the East and South Carpathians bearing ophiolites or displaying deep oceanic affinities. This let to the conclusion that the deep oceanic domain, which opened during the Jurassic (Oxfordian-Kimmerigian, the age of the oldest sediments and ophiolites) and was completely subducted after the Late Cretaceous compression (Săndulescu, 1988). This is evidenced by the limited extent of the Ceahlău-Severin ocean. This ocean is considered to be a branch of the Alpine Tethys, which only in the frontal part of the East and South Carpathians, possibly dissected by major transcurrent systems (Bădescu, 1997; Schmid et al., 2008). However, the basin continued to evolve throughout the Paleogene and Miocene in a thinned continental domain, often envisaged as a North Sea-type passive continental margin, which was gradually underthrust beneath the Bucovinian and Getic units.

5.2.4. Convolute Flysch/Audia/Macla nappe system

The Convolute Flysch nappe (Dumitrescu, 1952), the most internal unit of SE Carpathians (Fig. 5.2; Săndulescu et al., 1981) contains a Hauterivian-Senonian turbiditic series (Ştefănescu, 1976), which is gradually fining upwards, mainly located in the S and SW parts of the East Carpathians. The Macla nappe (Fig. 5.2; Popescu, 1958) is a narrow unit developed along the central and southern parts of the East Carpathians. It contains Albian-Senonian deposits developed in similar, but more distal facies than the Convolute Flysch nappe, indicating a similar depositional environment. The unclear offsets between these two nappes make their distinction rather difficult (Băncilă, 1958). The Audia nappe (Dumitrescu, 1952) can be followed at surface as far south as the Buzău valley, where it is supposedly tectonically overthrust by the more internal Macla/Convolute units (Fig. 5.2). It contains Barremian-Albian distal partly bituminous shales, which are overlain by coarser and proximal turbidites of Eocene age (Băncilă, 1958; Ionesi, 1971). Sediments have been apparently deposited in a different sedimentary environment along the horst and graben structures of the European passive continental margin, being partly sourced by a western uplifted area (i.e. "Cuman cordillerra"; Murgeanu, 1937), which separated the Audia nappe sediments from the more internal units (Săndulescu, 1988).

These nappes have been emplaced during the Early Miocene and are covered by the Lower Miocene post-tectonic deposits. They are best exposed in the S and SW termination of the East Carpathians (Ştefănescu, 1976). Along strike, the Audia nappe is largely exposed in the north, while the Macla nappe is only observed in the south. Despite the lack of kinematic studies in these units, their spatial arrangement suggests a NE-ward direction of thrusting, which is oblique to the N-S structural grain of the continental passive margin (Matenco and Bertotti, 2000).

5.2.5. Tarcău/Marginal Folds/Subcarpathian nappes

The Tarcău and Marginal Folds nappes (Dumitrescu, 1952) are composed of Cretaceous marine fine clastics (shales and marls), overlain by a turbiditic succession of Senonian-Upper Oligocene age, and a Lower Miocene molasse-type formation associated with salt deposition (Săndulescu et al., 1981 and references therein). The frontal unit, the Subcarpathian nappe is mainly made up of deeply buried Eocene to Oligocene clastics, overlain by the Miocene molasse-type sediments interbedded with two evaporitic levels of Burdigalian and Badenian age (Săndulescu, 1988). The thrusting of these nappes took place successively during the Middle and Late Miocene, kinematic directions varying from ENE-WSW in the central and northern part to ESE-WNW in the southern part of the East Carpathians (Morley, 1996; Ellouz et al., 1994; Ziegler et al., 1995; Matenco and Bertotti, 2000).

5.2.6. Regional context to Paleogene evolution: quiescence or potential shortening in the SE Carpathians?

The Late Cretaceous-Paleogene thrusting and transpression of the Balkans over the Moesian platform (Doglioni et al., 1996) was followed by the large scale rotations of the internal Carpathians (i.e. Tisza-Dacia unit) around the Moesian block during the Paleogene-Early Miocene (Csontos and Vörös, 2004; Fügenschuh and Schmid, 2005). The South Carpathians rotation was characterised by the Latest Cretaceous-Eocene orogen-parallel extension (Schmid et al., 1998; Matenco and Schmid, 1999; Fügenschuh and Schmid, 2005) and dextral movements along two curved fault systems, the Cerna-Jiu and Timok, respectively. The former accounts for 35 km dextral offset during the Oligocene (Berza and Drăgănescu, 1988), while the latter for 65 km dextral offset in the Early Miocene (Moser, 2001; Kräutner and Krstic, 2003). They are located near the present-day contact between the South Carpathians and the Getic Depression and resulted in the opening of an up to 3 km thick Lower Miocene basin (Răbăgia et al., submitted). The Paleogene shortening documented as well in the internal Carpathian units is represented by the reactivation of the Late Cretaceous faults located close to the contact between the Tisza and Dacia blocks (i.e. the Puini thrust) and/or to the contact between the Apuseni Mountains and Transylvanian basin (Krézsek and Bally, 2006; Schmid et al., 2008 and references therein).

Both Paleogene and Lower Miocene kinematics account for a NE-ward movement of the internal Carpathian units relative to the European foreland. Due to the curved shape of the orogen, the South Carpathians transcurrent movements can be coeval with the NE-vergent thrusting in the East Carpathians (see also Fügenschuh and Schmid, 2005). This is the case for the ~65 km Early Miocene transtension, which in the East Carpathians is coeval with the emplacement of the Convolute Flysch/Macla/Audia nappes on an ap-

parently compatible NE-ward direction.

However, the unknown amount of the Latest Cretaceous-Eocene extension along the South Carpathians strike, and the 35 km Oligocene dextral offset of the Cerna-Jiu fault do not have so far a time equivalent in the East Carpathians, where the Paleogene is interpreted so far as a period of relative quiescence. The Paleocene-Eocene asymmetric facies distribution (thicker and coarser to the west) has been speculated as an extensional period along potentially listric normal faults (Săndulescu, 1994). Such normal faults have not been observed so far in the thin-skinned wedge, and the facies distribution can be alternatively interpreted as a syn-tectonic foredeep wedge (senso Bertotti et al., 2003).

5.2.7. Post-collisional deformations across the SE Carpathians

The post-collisional (<11 Ma) evolution of the external Carpathian nappes and the adjacent foreland is characterized by two distinct periods (Necea et al., 2005; Leever et al., 2006; Matenco et al., 2007). A first, Latest Miocene-Pliocene (Late Sarmatian-Romanian) period of generalized subsidence which affected the entire domain and a second period represented by Quaternary folding of 5 km, respectively. Two mechanisms have been proposed to explain these deformation periods, the pull-down effect exerted by the subsiding Vrancea slab locked during the Late Miocene collision and the Quaternary inversion of the entire Carpathian-Pannonian system driven by the northward movement of the Adriatic indentor (Matenco et al., 2007), respectively. The contraction was active in a WNW-ESE oriented corridor delimitated by the Intramoesian fault in the SW and by the Trotuş and Peceneaga-Camena faults in the north and NE (Fig. 5.1).

Previous AFT data suggest that exhumation of 4 km took place north of the Trotuş fault during the Middle-Late Miocene (11-9 Ma in ; Sanders et al., 1999). In the southern part of the bending zone, i.e. Buzău valley (Fig. 5.3), up to 2 km of exhumation took place during the Pliocene-Quaternary, which caused isostatic uplift of this region (5-0 Ma; Sanders et al., 1999). Pliocene extension recorded in the internal orogenic nappes resulted in formation of few intramontane basins (Fig. 5.2b). An unusual foredeep basin, i.e. Focşani basin, developed in the frontal part of the bending zone since the Late Miocene continental collision (Fig. 5.2b). The exhumed orogen became probably source areas for this basin, where more than 10 km of sediments have been deposited during the Late Miocene-Quaternary (Fig. 5.2b). Presently, sedimentary deposits on the western flank of the Focşani basin are strongly tilted eastward (Fig. 5.2b), with dip ranging from 87° for the Sarmatian (Late Miocene) to 15° for the Romanian strata (Late Pliocene; Necea et al., 2005). This unusual tilting might be caused by strong deformation in the mountain chain coupled with subsidence in the basin centre .

During the Quaternary, deformation is indicated by the ENE-ward late Early Pleistocene tilting (Necea et al., 2005), Early Pleistocene E-W to NE-SW trending out-of-sequence thrusts and folds located south of the Buzău valley (Hippolyte and Săndulescu, 1996; Hippolyte et al., 1999; Matenco and Bertotti, 2000), Middle Pleistocene-Holocene numerous levels of river terraces placed at different elevations (Necea et al., 2005; Ghenea et al., 1971), angular unconformities visible in the field and on reflection seismic lines (Leever et al., 2006) and GPS studies (van der Hoeven et al., 2005).

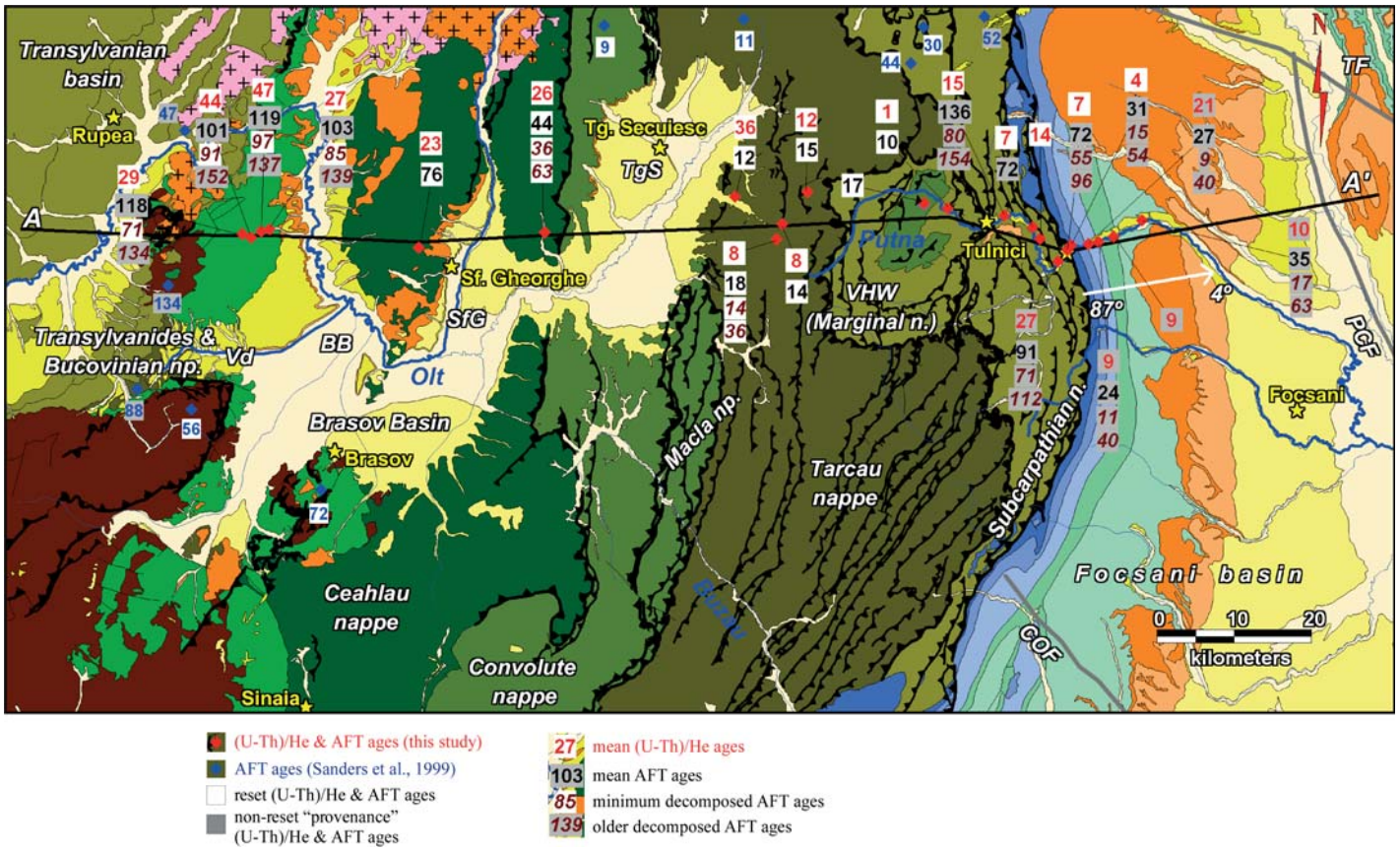

Figure 5.3

New AFT and (U-Th)/He data (red values) are plotted together with the previous published AFT data (blue values; Sanders et al., 1999) on the geological map. Notice that the mean AFT ages have been decomposed in two age groups: minimum and older ages (interpretation in text).

5.3. Low-temperature thermochronology

The 21 samples analysed for apatite fission-track (AFT) and (U-Th)/He methods have been collected along a 175 km long W-E-orientated transect. It starts westward in the Transylvanian hinterland basin, crosses the orogenic system and ends on the eastward tilted flank of the Focşani basin (Fig. 5.2b). All samples composed entirely of sedimentary rocks have been collected from different elevations, from 220 m for the Upper Pliocene strata of the Focşani basin to 1200 m for the Paleocene-Oligocene deposits of the Tarcău nappe. To the west, samples were taken from the Albian post-tectonic conglomeratic cover of the Bucovinian nappe, from the Aptian sandstones of the Baraolt nappe and from the Barremian-Albian sandstones of the Ceahlău nappe (Table 5.1). In the Convolute/Audia/Macla nappes, sampling was hampered by the overlaying Pliocene-Quaternary volcanic-sedimentary sequence in the Braşov basin. Eastward in the external nappes, samples were taken from the Paleocene-Oligocene sandstones of the Tarcău nappe, from the Cretaceous conglomerates of the Marginal Folds nappe, from the Middle Miocene (Burdigalian) conglomerates and sandstones of the Subcarpathian nappe, and additionally from each stratigraphic interval of the Uppermost Miocene-Pliocene strata in the Focşani basin (Table 5.1, with sample locations in Fig. 5.2a).

AFT and *(U-Th)/He analytical results* exhibit significant variance probably because the individual apatite grains have non-uniform sources and/or experienced different cooling histories. The results are shown in Table 5.1 and Fig. 5.2a. The AFT ages range from 119±12 to 10±2 Ma (Figs. 5.3 and 5.8a,c). He ages have been determined on the same samples analyzed for AFT and are comprised between of 47±4 and 1±0 Ma (Figs. 5.3 and 5.8b,c).

AFT data are interpreted using the Chi-squared probability test (Galbraith, 1981; Green, 1981), which is a statistical deconvolution of sample grain-age distributions (Brandon, 1992; Brandon and Vince, 1992) and inverse thermal modelling (Ketcham et al., 1999), which is based on AFT and He ages, track lengths, size of etch-pits (D-par) and two geological constraints (explained in Subchapter 5.4.). The $P\chi^2$ test classifies the grain-age distribution as either concordant with $P(\chi^2)>5\%$ (samples passed the test), or discordant with $P(\chi^2)<5\%$ (samples did not pass the test; Galbraith, 1981; Green, 1981). Concordant samples yield one age which is equivalent to the pooled age. Discordant samples display multiple age components and central age has to be used (Galbraith and Laslett, 1993). Better is to identify (1) the minimum age component which not only constrains the most recent cooling, but also can be used as a proxy for deposition in non-reset samples (Brandon and Vance, 1992; Garver et al., 1999), and (2) the older age component which can be associated with either a more thermally resistant apatite and/or with a different source area (Carlson et al., 1999). Based on these distinctions, the ages can be separated as reset (younger than stratigraphy) and non-reset samples (older than stratigraphy).

Majority of the AFT samples from this study did not pass the $P(\chi^2)$ test (Table 5.1), which imply that the age distribution is composed of several age components. Few samples yield AFT ages younger than the stratigraphy and passed the test (Table 5.1). Single grains from each of these samples might have experienced the same degree of annealing post-deposition. All ages younger than stratigraphy can be interpreted in terms of burial and subsequent cooling/exhumation that followed after deposition. The other obtained ages yield generally pre-depositional non-reset mixed-ages. These ages provide informa-

Figure 5.4

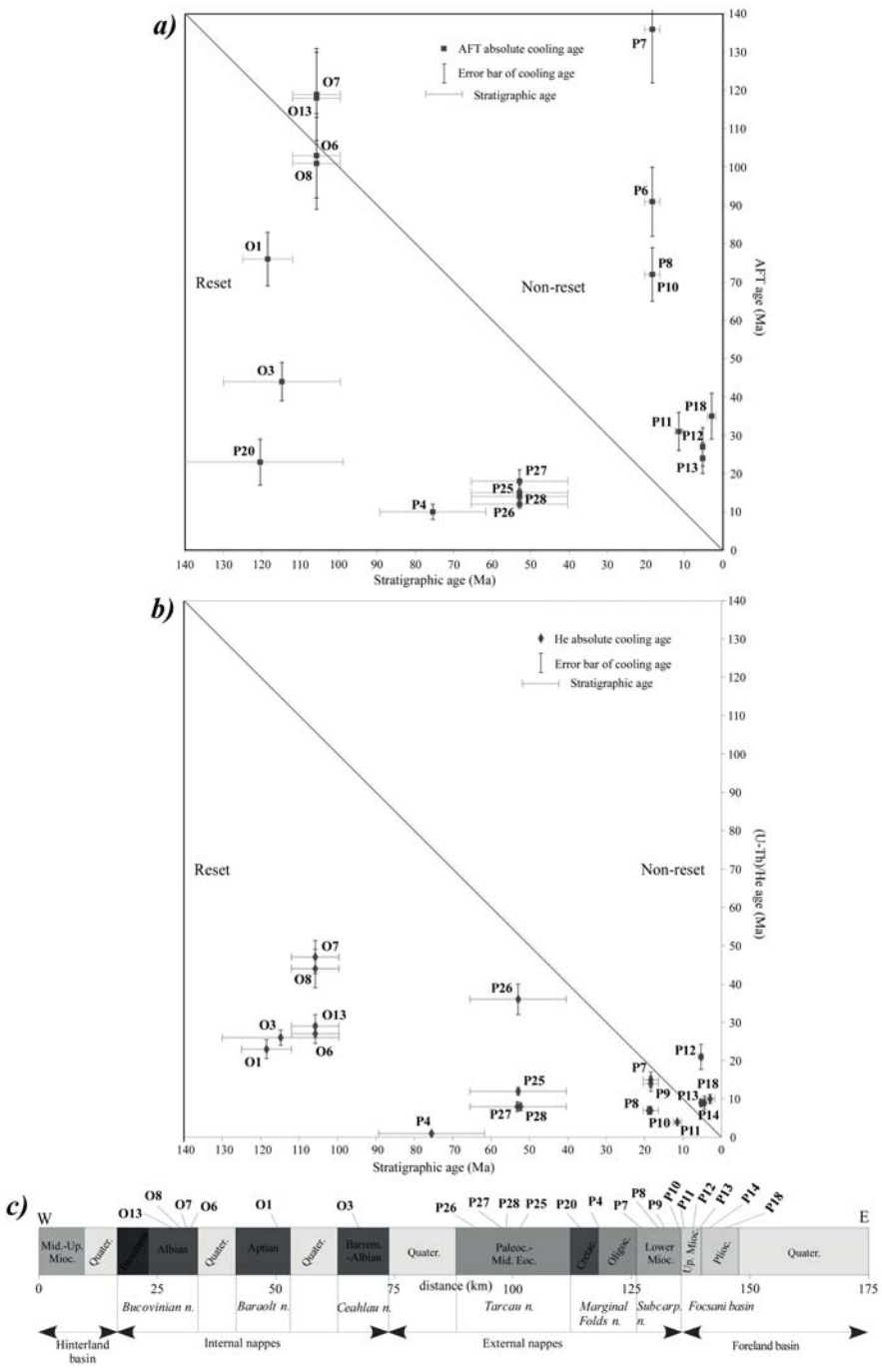

AFT data plotted vs. stratigraphy. Reset and non-reset ages have been equally recorded in the internal and external orogenic units, the non-reset values predominating eastward in the Upper Miocene-Pliocene sediments of the Focşani foreland basin. (b) (U-Th)/He data plotted vs. stratigraphy. Reset ages have been obtained in the internal and external units and deeper sediments of the Focşani basin, while non-reset ages have been recorded only in the Uppermost Miocene-Pliocene sediments of the Focşani basin. (c) Sample codes from different geological units are distributed from west to east.

tion on the cooling/exhumation history of one or multiple source areas.

Samples from the foreland basin yielded large age dispersion, values of 60-80%, while lower values were recorded in the orogenic units (18-54%; Table 5.1). Large over dispersion might be due to the presence of several age populations. Therefore, a single age for the population is irrelevant. In the case of the obvious evidence of the large age dispersion, the pooled age and Poisson standard error are not applicable (Galbraith and Laslett, 1993) and instead, the central ages are used. These central ages with 1 sigma error (Ma) are presented in Table 5.1.

The Binomfit program was used for those samples where mixed-age distributions were indicated by the P(χ2) test (Table 5.1; Brandon, 1992). The results revealed two or three components for each sample, shown as age clusters in a radial plot (Galbraith and Laslett, 1993; values in Table 5.1 and Fig. 5.5). The minimum (youngest) component is much younger than stratigraphy for reset samples, much older for part of the non-reset samples and slightly younger for the other non-reset samples (i.e. Bucovinian nappe; Table 5.1). The older age components are used for provenance study.

He analytical results might yield similar variance as the AFT data because individual apatites might have non-uniform sources, different cooling histories, variable U and Th zonations (not analyzed in this study), different degrees of radiation damage, presence of undetectable fluid and solid inclusions (Ehlers and Farley, 2003). The limited number of 2 to 5 single grain He ages and the large age dispersion per sample prevented to model the age evolution curves with DECOMP program. However, the He ages together with the AFT data have been used for modelling performed with HeFTy program.

5.4. Thermal modelling approach

Thermal history and overall kinematics of the SE Carpathian orogen and its relationship with the adjacent basins were reconstructed from modelling the time-Temperature (t-T) paths of rocks collected from the source (orogenic) and sink (basinal) areas. Inverse t-T models were calculated with HeFTy program (Ketcham, 2005), which uses an iterative (Monte Carlo) numerical approach. The t-T constraints (boxes) used in this study are: stratigraphy, AFT and (U-Th)/He ages (including track length distributions and etch-pit measurements), two regional geological constraints (Oligocene exhumation and Pliocene subsidence, respectively) and present-day surface temperature (Fig. 5.6). These constraints help defining boxes (t-T ranges) that the program must consider when model the t-T paths.

5.4.1. Geological constraints (boxes) and their limitations

Stratigraphical constraint was taken from the published data, i.e. from Patrulius et al. (1968) for samples from the Bucovinian, Baraolt and Ceahlău nappes, from Saulea et al. (1968) for samples from the Tarcău, Marginal Folds and Subcarpathian nappes and from the Focşani basin (here, also from Vasiliev et al., 2004).

AFT and (U-Th)/He age constraints that were used in modelling were described in Subchapter 5.3.

Oligocene exhumation constraint is based on coeval events recorded in the adjacent regions, previously not addressed in the SE Carpathians. These events are: Late Oligo-

cene-Early Miocene exhumation in the South Carpathians due to dextral transtention along the Timiş-Cerna and Timok faults (Bojar et al., 1998; Fügenschuh and Schmid, 2005; Schmid et al., 2008), Late Oligocene shortening in the western part of the Transylvanian basin, e.g. Puini thrust (Krézsek and Bally, 2006), Upper Cretaceous/Eocene-Oligocene erosional unconformity in the Vlădeni corridor of the Braşov basin (Săndulescu, 1972), Eocene/Middle Miocene (Badenian) unconformity in the Black Sea basin (Dinu et al., 2005), Paleogene sinistral transpression and Neogene dextral transtension along subvertical faults (e.g. Emine line) in the Eastern Balkans and their continuation into the Black Sea basin (Doglioni et al., 1996).

The Pliocene subsidence constraint is evidenced by palinspastic reconstructions of the post-collisional deformation and on biostratigraphic indicators that suggest an open water connection between the Braşov intamontane and the Focşani foreland basins, which requires that Pliocene subsidence affected the orogenic nappes (Leever et al., 2006).

Present-day surface temperature constraint was approximated to the annual average value, which in Romania is around 10°C.

These constraints (boxes) were kept relatively wide in most runs (~100.000-150.000 per sample) to give flexibility to the HeFTy program to search for possible solutions over a wide t-T space. The temperature limits correspond mainly to the PAZ and HeRZ (110-60°C and 75-40°C, respectively), while the time limits were randomly chosen at the beginning of modelling (however larger than the error bars), progressively maximized or minimized until the best fitting model was obtained (Fig. 5.9a). If these constrains were not enlarged enough, then the program would have been limited to model only using the constraints themselves. In particular for sample P4, t-T boxes were kept large enough, below the closure temperatures (110 and 75°C, respectively), in order not to limit the areas in which the modelling program will iterate.

In a first attempt, thermal modelling was performed including He single grain ages. The results gave neither acceptable nor good paths probably due to large spread in individual ages (Fig. 5.7b), and therefore, these results were not discussed further in this study. The t-T models improved considerably when mean He ages were used (Fig. 5.9a). In particular in the Bucovinian nappe, the AFT ages could not be successfully integrated in thermal modelling because some of them are similar to stratigraphy. Instead, minimum ages have been carefully used because they indicate that the samples entered in the PAZ and experienced partial resetting. The other studied samples show a differential pattern of burial and cooling (Fig. 5.9a). This is because several samples are older (i.e. Cretaceous) than others (i.e. Miocene), most likely they experienced separate thermal histories, with a different degree of annealing in accordance with their relative depth.

Three different t-T scenarios can result from thermal modelling of sediment samples: (1) samples with thermal histories which show temperatures below the closure temperature of the AFT system (<50°C), not applicable in this study; (2) samples which were buried entering in the PAZ and experienced partial annealing of the fission-tracks, i.e. samples from the Bucovinian nappe (O6, O7, O8 and O13); and (3) samples that experienced reheating at temperatures higher than those of the PAZ, leading to the total annealing of the fission-tracks and apply to all remaining samples (Fig. 5.9a).

During modelling, HeFTy program introduced “a younger Pliocene-Quaternary cooling artifact”, which is indicated by the He age which does not fit within the good t-T envelope (purple) or sometimes is close to the acceptable one (green). This artifact might

Figure 5.5

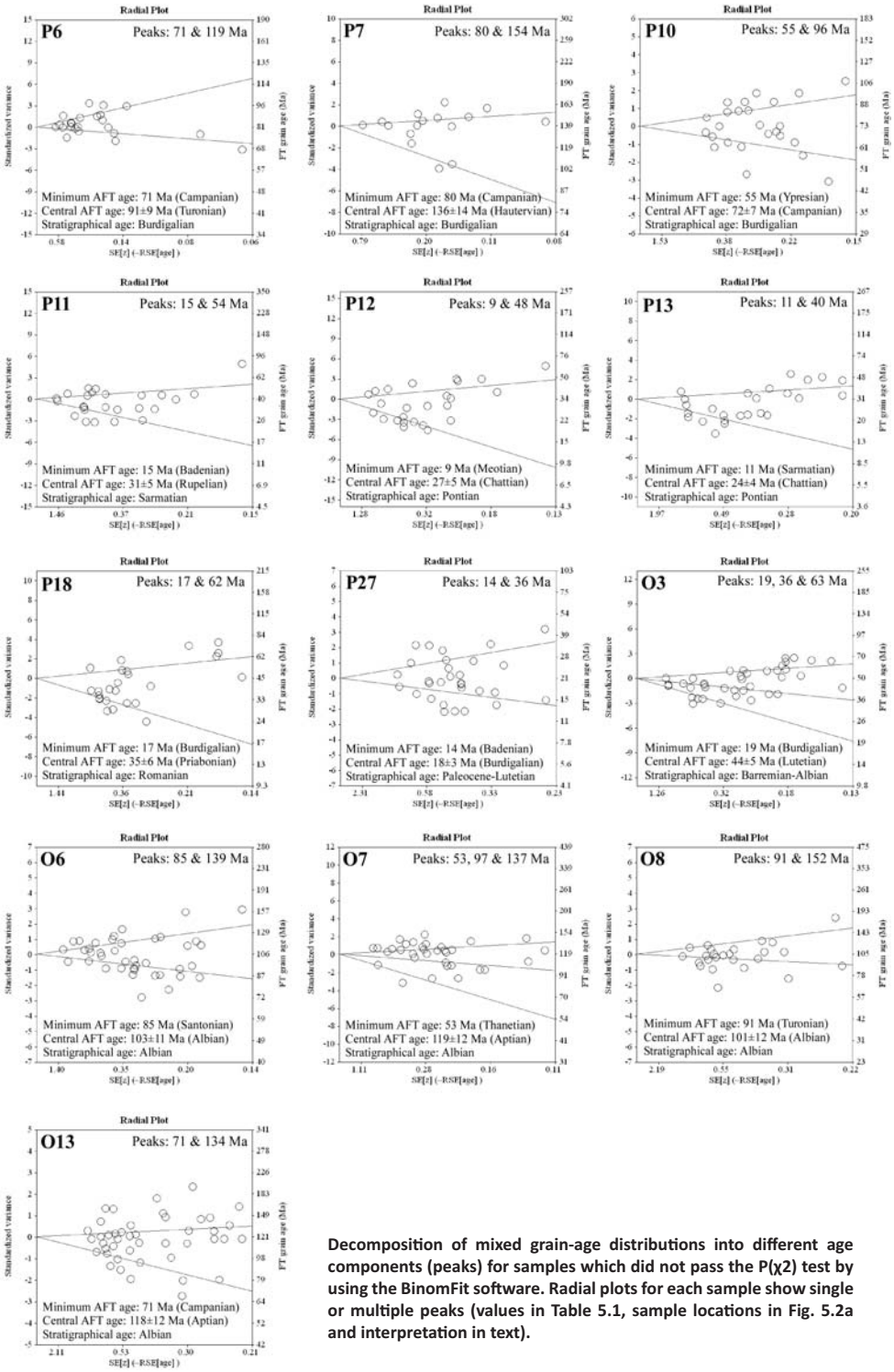

Decomposition of mixed grain-age distributions into different age components (peaks) for samples which did not pass the P(χ2) test by using the BinomFit software. Radial plots for each sample show single or multiple peaks (values in Table 5.1, sample locations in Fig. 5.2a and interpretation in text).

be due to the track length distribution (shorter tracks) and He age which indicates older cooling. It is known that fission-tracks still experience annealing at low temperature

Table 5.2

Sample name	Tectonic unit	Time interval	Constrain time max. (Ma)	min	diff.	Constrain temp start (°C)	end	diff.	Temp. - error bars min.	max. (°C)	diff.	Exhum.(+ /Burial(-) (km)	Error bar	Rate (mm/ yr)	Error bar	Tect. evolut.
O1	Baraolt np.	Aptian-Early Albian	125	105								stratigr.				S(D)
O1	Baraolt np.	Late Albian-Cenomanian	105	93	12	20	82	62	77	85	8	3.1	±0.5	0.3	±0.04	B(S)
O1	Baraolt np.	Turonian-Latest Chattian	93	23	70	82	58	24	77/40	85/75	8./35	1.2	±1.1	0.02	±0.01	SC-PAZ
O1	Baraolt np.	Latest Chattian-Dacian	23	5	18	58	10	48	40	75	35	2.4	±1.7	0.12	±0.09	FC(E)
O1	Baraolt np.	Dacian-Holocene	5	0												UC/B
O3	Ceahlau np.	Barremian-Early Albian	130	105								stratigr.				S(D)
O3	Ceahlau np.	Late Albian-Cenomanian	105	93	12	20	85	65	78	90	12	3.2	±0.6	0.3	±0.04	B(S)
O3	Ceahlau np.	Turonian-Chattian	93	27	66	85	58	27	78/40	90/75	12./3	1.4	±1.2	0.02	±0.02	SC-PAZ
O3	Ceahlau np.	Chattian-Dacian	27	5	22	58	10	48	40	75	35	2.4	±1.7	0.1	±0.07	FC(E)
O3	Ceahlau np.	Dacian-Holocene	5	0												UC/B
O6	Bucovinian np.	Late Albian-Cenomanian	105	93								stratigr.				S(D)
O6	Bucovinian np.	Late Albian-Cenomanian	105	93	43	20	87	67	82	90	8	3.4	±0.5	0.3	±0.04	B(S)
O6	Bucovinian np.	Turonian-Rupelian	93	29	64	87	68	19	82/59	90/77	8./18	1.0	±0.7	0.02	±0.05	SC-PAZ
O6	Bucovinian np.	Rupelian-Dacian	29	5	24	68	10	58	59	77	18	2.9	±0.9	0.12	±0.04	FC(E)
O6	Bucovinian np.	Dacian-Holocene	5	0												UC/B
O13	Bucovinian np.	Late Albian-Cenomanian	105	93								stratigr.				S(D)
O13	Bucovinian np.	Late Albian-Cenomanian	105	93	12	20	80	60	76	85	9	3.0	±0.4	0.3	±0.03	B(S)
O13	Bucovinian np.	Turonian-Chattian	93	27	66	80	72	8	76/66	85/69	9./13	0.4	±0.5	0.01	±0.007	SC-PAZ
O13	Bucovinian np.	Chattian-Dacian	27	5	22	72	10	62	66	79	13	3.1	±0.7	0.14	±0.03	FC(E)
O13	Bucovinian np.	Dacian-Holocene	5	0												UC/B
Mean	Bucovinian np.	Late Albian-Cenomanian	105	93								stratigr.				S(D)
Mean	Bucovinian np.	Late Albian-Cenomanian	105	93								3.2	±0.5	0.3	±0.04	B(S)
Mean	Bucovinian np.	Turonian-Chattian	*93*	*28*								*0.7*	*±0.6*	*0.01*	*±0.03*	SC-PAZ
Mean	Bucovinian np.	Chattian-Dacian	28	5								3.0	±0.8	0.13	±0.04	FC(E)
Mean	Bucovinian np.	Dacian-Holocene	5	0												UC/B
P4	Marginal F. np.	Coniacian-Danian	89	62								stratigr.				S(D)
P4	Marginal F. np.	Danian-Early Burdigalian	62	18	44	20	122	102	115	130	15	5.1	±0.9	0.1	±0.02	B(S)
P4	Marginal F. np.	Early Burdig.-late Early Pleist	18	1.5	16.5	122	105	17	115/102	130/109	15./7	0.9	±0.6	0.05	±0.03	SC-PAZ
P4	Marginal F. np.	late Early Pleist.-Holocene	1.5	0	1.5	105	10	95	102	109	7	4.8	±0.4	3.2	±0.3	FC(E)
P7*	Subcarpathian np.	Burdigalian	20	16								stratigr.				S(D)
P7*	Subcarpathian np.	Early Badenian	16	14		20	75					2.8	±0.4	1.4	±0.02	B(S)
P7*	Subcarpathian np.	Late Badenian-Holocene	14	0		75	10					3.2	±0.5	0.2	±0.03	FC(E)
P8*	Subcarpathian np.	Burdigalian	20	16								stratigr.				S(D)
P8*	Subcarpathian np.	Earliest Badenian-Meotian	16	7		20	75					2.7	±0.4	0.3	±0.04	B(S)
P8*	Subcarpathian np.	Meotian-Holocene	7	0		75	10					3.2	±0.5	0.5	±0.08	FC(E)
Mean	Subcarpath. np.	Burdigalian	20	16								stratigr.				S(D)
Mean	Subcarpath. np.	Badenian-Sarmatian	16	11								2.8	±0.4	0.9	±0.03	B(S)
Mean	Subcarpath. np.	Sarmatian-Holocene	11	0								3.2	±0.5	0.3	±0.06	FC(E)
P11*	west Focsani bs.	Sarmatian	13	11								stratigr.				S(D)
P11*	west Focsani bs.	Late Sarmatian-Romanian	11	4								2.8	±0.4	0.4	±0.06	B(S)
P11*	west Focsani bs.	Romanian-Holocene	4	0								3.2	±0.5	0.8	±0.1	FC(E)
P25	Tarcau np.	Danian-Lutetian	65	40								stratigr.				S(D)
P25	Tarcau np.	Lutetian-Aquitanian	40	23	17	20	97	77	90	105	15	3.8	±0.7	0.2	±0.04	B(S)
P25	Tarcau np.	Aquitanian-Holocene	23	0	23	97	10	87	90	105	15	4.3	±0.7	0.2	±0.03	FC(E)
P26	Tarcau np.	Danian-Lutetian	65	40								stratigr.				S(D)
P26	Tarcau np.	Lutetian-Late Burdigalian	40	17	23	20	99	79	90	105	15	4.0	±0.8	0.2	±0.03	B(S)
P26	Tarcau np.	Late Burdigalian-Holocene	17	0	10	99	10	89	90	105	15	4.4	±0.8	0.3	±0.05	FC(E)
P27	Tarcau np.	Danian-Lutetian	65	40								stratigr.				S(D)
P27	Tarcau np.	Lutetian-Early Burdigalian	40	20	20	20	100	80	95	105	10	4.0	±0.5	0.2	±0.03	B(S)
P27	Tarcau np.	Early Burdigalian-Holocene	20	0	20	100	10	90	95	105	10	4.5	±0.5	0.2	±0.02	FC(E)
Mean	Tarcau np.	Danian-Lutetian	65	40								stratigr.				S(D)
Mean	Tarcau np.	Lutetian-Early Burdig.	40	20								3.9	±0.7	0.2	±0.03	B(S)
Mean	Tarcau np.	Early Burdigalian-Holocene	20	0								4.4	±0.7	0.2	±0.03	FC(E)

Burial and cooling amounts and rates calculated for representative samples. Burial and cooling intervals were defined between two inflection points along either good t-T paths or forward sketches for each sample (intervals in Fig. 5.9a). Three formulas were introduced to calculate these values (Subchapter 5.4.2). Notice that the two or three analysed samples in the Bucovinian, Tarcău and Subcarpathian nappes were summed together and mean values per unit were used to reconstruct the geological evolution. In samples P7, P8 and P11, the computed amounts and rates are maximum estimations because inverse modelling could not be performed (discussion in text). UC/B-Undifferentiated cooling/burial, FC(E)-Fast cooling (exhumation), SC-PAZ-Slow cooling in Partial Annealing Zone, B(S)-Burial (subsidence) and S(D)-Stratigraphy (deposition).

(<60°C) and over millions of years (Green at al., 1989; Donelick et al., 1990), both are not fully integrated in thermal modelling. One way to deal with this artifact is to use an initial track length shorter than 16.3 µm (Ketcham et al., 2000), but because this might involve additional correction measures, it was neglected during this study. Regardless of this artifact, forward modelling was performed, which also included the He age. The cooling history provided by the He age is critical for obtaining the 1-2 km of typical exhumation taking place during the nappe thrusting events. The He cooling part of the burial-cooling curve is better illustrated by the forward modelling (samples O1, O3, P25-P28). Foreword modelling was also done for those samples that could not be inversely modelled due to non-reset AFT age and lack of track length measurements (samples P7, P8 and P11). The coloured areas (envelops) of models presented in Fig. 5.9a stand for: purple for good paths, green for acceptable paths, while the best fitting path is shown as a dashed black line.

Well-constrained thermal models have been obtained for seven of the 21 samples, which yielded both AFT and He reset ages (Table 5.1. and Fig. 5.9). In the Bucovinian nappe, models of samples O7 and O8 display a *young cooling artifact*, as shown by the smaller values of the good of fitting between the measured and modelled AFT ages and track lengths, these models were neglected from interpretation. Models of samples O6 and O13 from the same nappe have been chosen as representative models because of the good reproducibility, the He ages being nicely included within the good t-T envelop. Models of samples O1 and O3 from the Baraolt and Ceahlău nappes, respectively, show

Figure 5.6

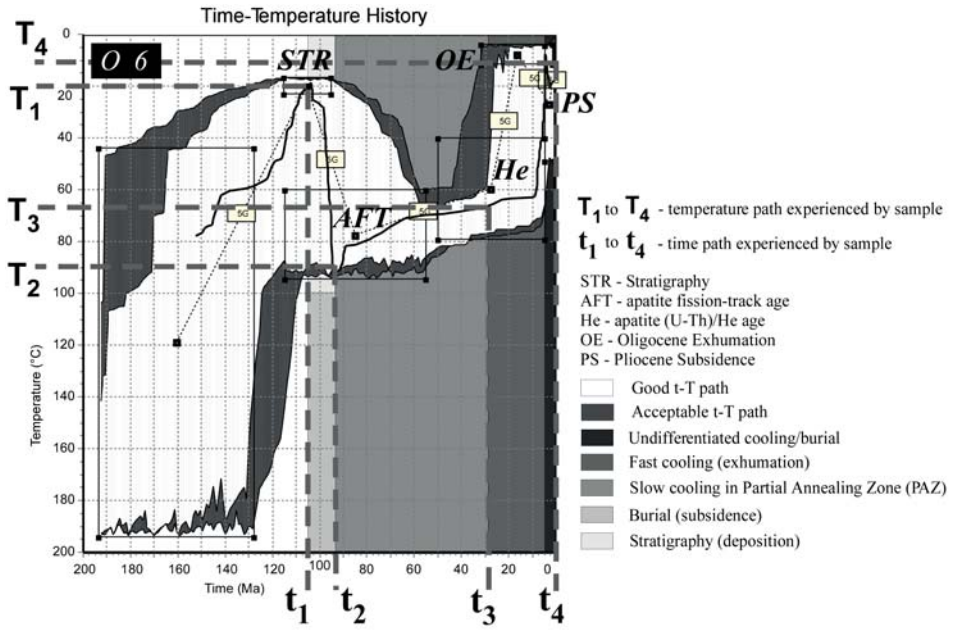

Example of time-Temperature intervals separated between two inflection points along the t-T path of sample O6 (i.e. burial, slow cooling corresponding to PAZ and fast cooling) used to determine the maximum (T2) and intermediate (T3) paleotemperatures experienced by this sample and the corresponding times (t2 and t3). These values were used to calculate the burial and cooling amounts and rates, with error bars (values in Table 5.2 and interpretation in Subchapters 5.5 and 5.6).

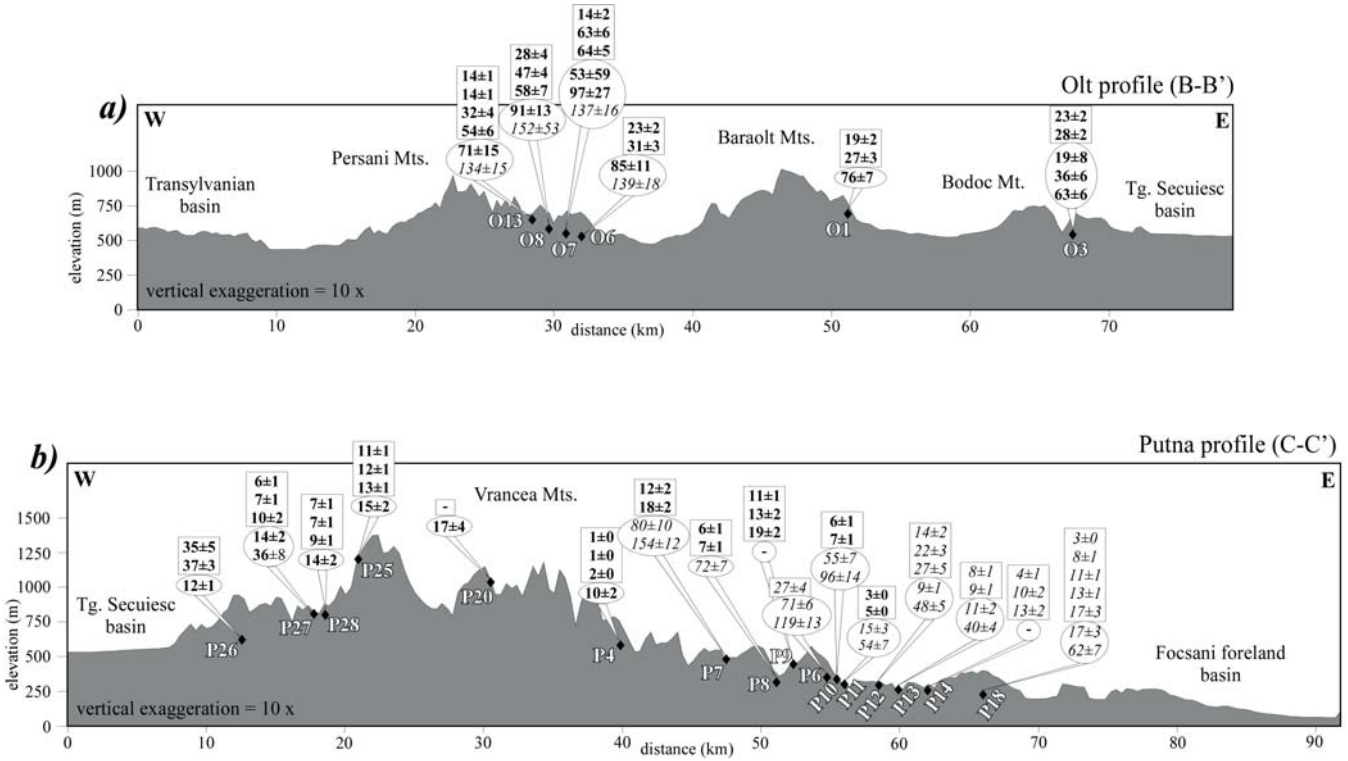

Single analysis α-corrected (U-Th)/He ages (in rectangles) and peaks of decomposed AFT ages (in circles) are plotted vs. elevation along the topographic profiles of the Olt (a) and Putna (b) valleys (B-B' and C-C' profiles in Fig. 5.2a). The bold values correspond to reset ages, while italic values are non-reset ages (provenance) for (U-Th)/He and AFT (values in Table 5.1). Notice that AFT ages are missing in samples P9 and P14 because they were not measured, while other samples display only one age (pooled age) because they passed the P(χ2) test. The He age missing in sample P20 is due to lack of good apatite grains, while in sample P26 the He age is older than the AFT age and is probably due to wrong measurements, this sample was used as a test sample.

Figure 5.8

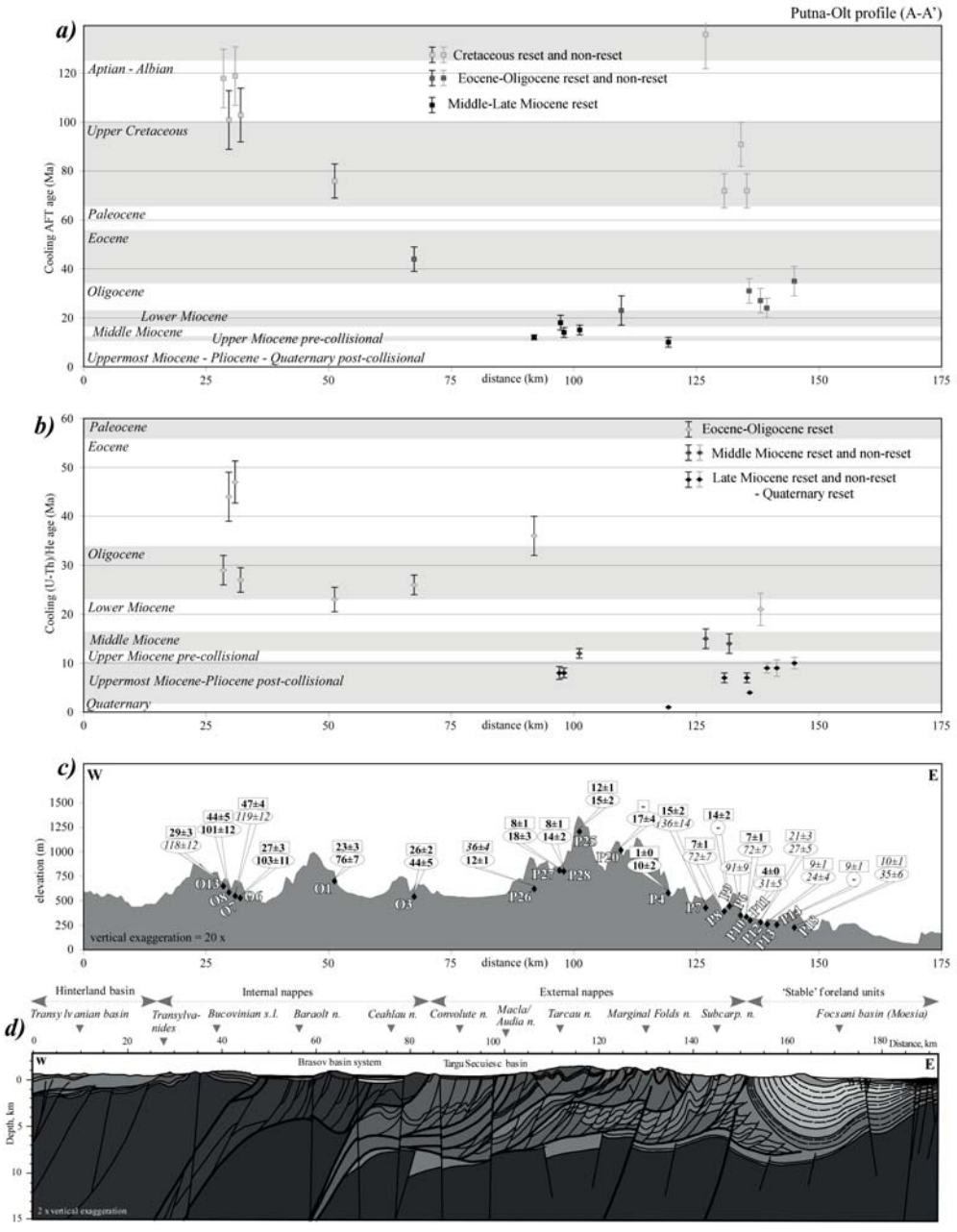

AFT (a) and apatite (U-Th)/He (b) ages are plotted vs. elevation (c) and geology (d) along the Putna-Olt profile (A-A' in Fig. 5.2a). (c) Rectangles and circles show the mean AFT and (U-Th)/He, respectively. AFT ages were not measured in samples P9 and P14. The He ages are missing in sample P20 due to lack of good apatites and in sample P26 due to wrong measurements. The bold values correspond to reset ages, while italics to non-reset ones (provenance). (d) Regional geological cross-section is modified after Schmid et al. (2008) and Leever et al. (2006). Data discussion and interpretation in text.

also the *young cooling artifact*. However, forward modelling was performed for each sample and was used in thermal reconstruction because there is only one sample per nappe.

In the Tarcău nappe, model of sample P26 done without He age (because of poor results) indicate the same thermal pattern as samples P25, P27 and P28. Although all four models indicate the *young cooling artifact* as in the internal western nappes, forward models illustrate better the last part of cooling. Model of sample P28 was neglected because of higher discrepancy between the inverse and forward modelling. Forward models of samples from the Subcarpathian nappe and the western flank of the Focşni basin illustrate the potential thermal histories.

5.4.2. Revealing the burial and cooling amounts, rates and error bars

The total amounts of burial and cooling predicted from HeFTy t-T modelling are, beside the AFT and (U-Th)/He input data, also a dependant on assumptions of surface temperature and paleotemperature gradient. A surface temperature of 10°C/km and a geothermal gradient of 20°C/km were assumed. The geothermal gradient has been derived by Sanders (1998), who balanced erosion along the Carpathian chain and Apuseni mountains against the sedimentary infill of the Transylvanian basin. This gradient is also in accordance with the present-day temperature measurements performed in wells from the external nappes and on the western flank of the Focşni basin (Demetrescu et al., 2005; Demetrescu et al., 2007) and with the present-day heat flow data recorded across the orogen (Veliciu and Visarion, 1984; Demetrescu and Veliciu, 1991; Demetrescu and Andreescu, 1994). Reconstruction of the paleogeothermal gradient was not possible during this study because vertical topographic profiles could not be found in the field due to low topography and vegetation, and unavailability of well data.

Furthermore, the temperature gradient might have been perturbed by the Late Miocene-Quaternary alkaline volcanism that affected regionally the internal orogenic nappes (Seghedi et al., 2004, 2005). However, the age of this volcanism in the study area is too young (<10 Ma; Late Miocene-Quaternary) to induce thermal resetting of the AFT and He ages. These ages were not affected by the volcanism as they are much older than the volcanism, i.e. AFT ages: Cretaceous to Eocene and (U-Th)/He ages: Eocene to Oligocene, respectively.

The surface temperature, geothermal gradient, modelled maximum and intermediate paleotemperatures experienced by the rock sample and the corresponding times were used to calculate the burial and cooling amounts. These were calculated for certain t-T intervals separated between two inflection points along the t-T path of each sample (i.e. burial, slow cooling corresponding to PAZ and fast cooling; Fig. 5.6 and Table 5.2). Three formulas were introduced to calculate the burial and cooling amounts (5.4.1), rates (5.4.2) and error bars (5.4.3).

The burial and cooling amounts were calculated as follows:

$$A_b = \frac{(T_2 - T_1)}{G} \qquad A_{c1} = \frac{(T_2 - T_3)}{G} \qquad A_{c2} = \frac{(T_3 - T_4)}{G} \tag{5.4.1.}$$

where: A_b, A_{c1}, and A_{c2} are the amounts of burial, slow cooling (in PAZ) and fast cooling

Figure 5.9 (1/3)

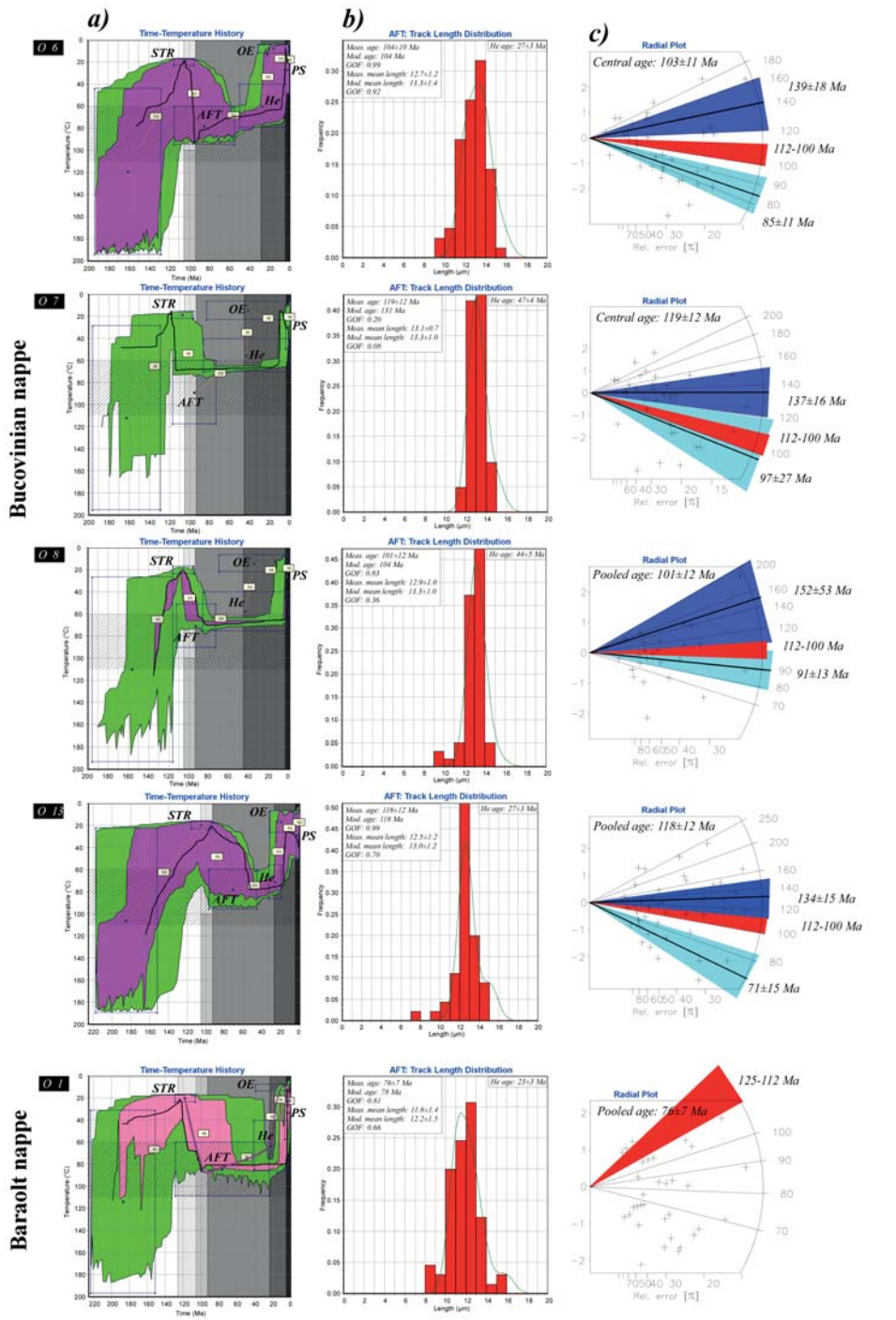
a)
b)
c)
Bucovinian nappe
Baraolt nappe
O 6
O 7
O 8
O 13
O 1
Time-Temperature History
AFT: Track Length Distribution
Radial Plot
STR
OE
PS
He
AFT
Central age: 103±11 Ma
139±18 Ma
112-100 Ma
85±11 Ma
Central age: 119±12 Ma
137±16 Ma
112-100 Ma
97±27 Ma
Pooled age: 101±12 Ma
152±53 Ma
112-100 Ma
91±13 Ma
Pooled age: 118±12 Ma
134±15 Ma
112-100 Ma
71±15 Ma
Pooled age: 76±7 Ma
125-112 Ma
Undifferentiated cooling/burial
Fast cooling (exhumation)
Slow cooling in Partial Annealing Zone (PAZ)
Burial (subsidence)
Stratigraphy (deposition)
Good t-T path
Acceptable t-T path
Forward t-T path
STR - Stratigraphy
AFT - apatite fission-track age
He - apatite (U-Th)/He age
OE - Oligocene Exhumation
PS - Pliocene Subsidence
AFT-PAZ - apatite fission-track Partial Annealing Zone
Stratigraphical age
Minimum decomposed age
Maximum decomposed age

Figure 5.9 (2/3)

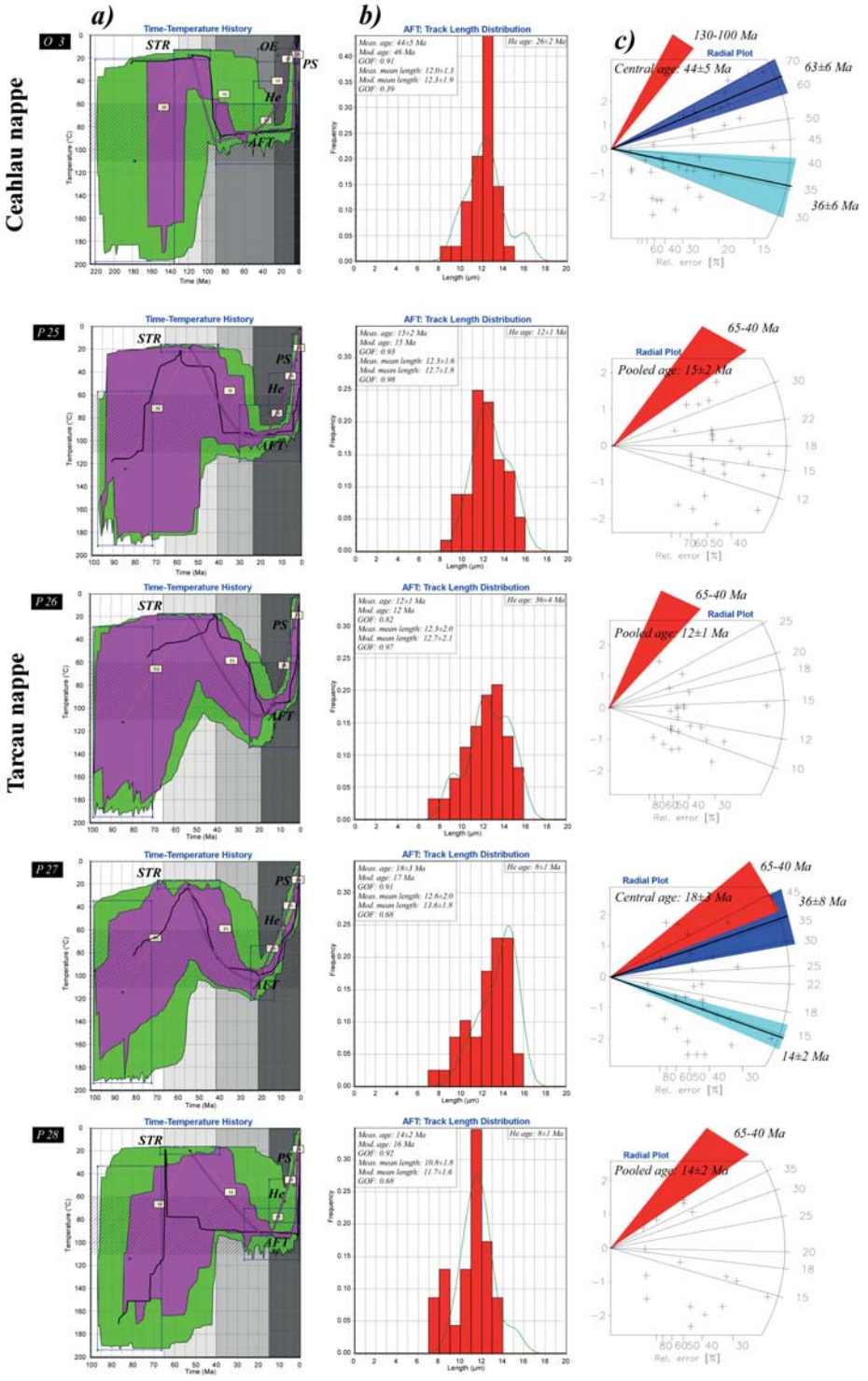
a)
b)
c)
Ceahlau nappe
Tarcau nappe
O 3
P 25
P 26
P 27
P 28
Time-Temperature History
AFT: Track Length Distribution
STR
OE
PS
He
AFT
Time (Ma)
Temperature (°C)
Length (µm)
Frequency
130-100 Ma
Radial Plot
Central age: 44±5 Ma
63±6 Ma
36±6 Ma
65-40 Ma
Pooled age: 15±2 Ma
Pooled age: 12±1 Ma
Central age: 18±3 Ma
14±2 Ma
Rel. error [%]

Figure 5.9 (3/3)

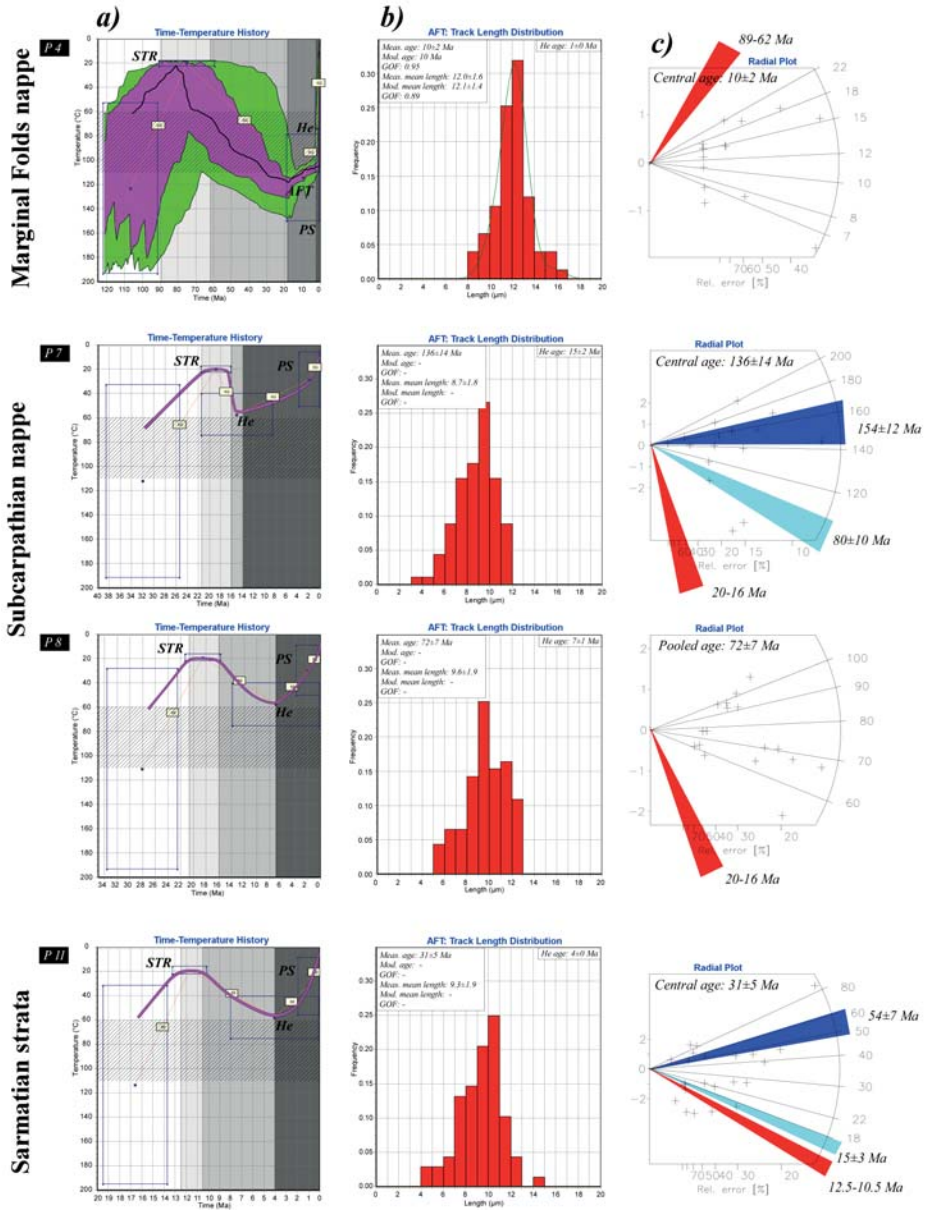

(a) Thermal history modelling of the SE Carpathian samples were performed with HeFTY software (Ketcham, 2005). The best fit thermal history is depicted as a black thick line within the purple envelop (good path). Notice that forward models were computed for samples P7, P8 and P11 because inverse modelling could be done due to non-reset AFT ages. Models of samples O1, O3 and P25 to P28 present also forward models beside the modelled t-T paths because mean He ages could not be incorporated in modelling. Samples O1, O3, O6 to O8, O13, P4, P7, P8, P11 and P25 to P27 have been chosen for interpretation. Time-temperature intervals used to calculate the burial and cooling amounts and rates are defined between two inflection points of either inverse or forward models (values in Table 5.2). Colours from models stand for: light-green for acceptable t-T path, light-purple for good t-T path and dark-purple for forward t-T path. (b) Track length distributions used for inverse modelling, with measured/modelled AFT age, measured/modelled mean lengths, good of fitting (GOD) and He age. (c) Radial plots show single grain AFT ages counted for each sample. For all samples which passed the P(χ2) test, the pooled age is reported, while for those which did not pass with P(χ2) <5%, the central age is used and decomposed ages are also reported. The coloured intervals stand for: red for stratigraphy, light-blue for minimum decomposed AFT age and dark-blue for maximum decomposed AFT age. Error bars are in Ma with ±1 sigma error.

(km) experienced by the sample. T_1 is the surface temperature (°C) at sample deposition (stratigraphy), T_2 is the maximum paleotemperature (°C) reached by the sample and corresponds to AFT age, T_3 is an intermediate paleotemperature (°C) reached by sample when passed through the He retention zone (U-Th/He age) and T_4 is the present-day surface temperature approximated at 10°C. G is the geothermal gradient of 20°C/Km.

The burial and cooling rates were determined using formula:

$$R_b = \frac{A_b}{(t_1 - t_2)} \qquad R_{c1} = \frac{A_{c1}}{(t_2 - t_3)} \qquad R_{c2} = \frac{A_{c2}}{(t_3 - t_4)} \tag{5.4.2.}$$

where: R_b, R_{c1}, and R_{c2} are the rates for burial, slow cooling (in PAZ) and fast cooling (mm/yr). t_1 is the sample deposition time (stratigraphy; Ma), t_2 is the time when the sample experienced the maximum burial given by the AFT age (Ma), t_3 is the time when the sample passed the He system corresponding to the (U-Th/He age; Ma) and t_4 is the

Figure 5.10

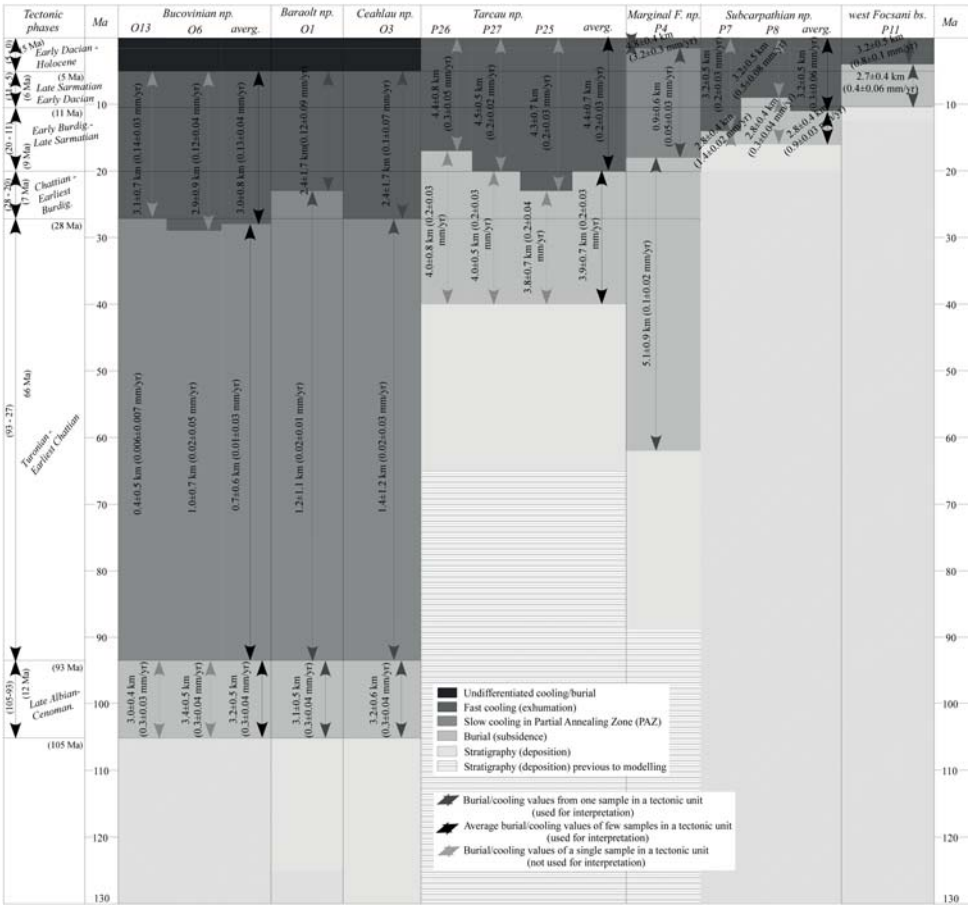

Correlation of individual deformation stages identified in each nappe, based on which seven tectonic phases have been identified (1-7 in Fig. 5.11), as described in the text. Notice that the burial/exhumation amounts and rates for the Subcarpathian nappe and the Sarmatian strata of the Focşani basin are only rough estimations.

present-day time.

The error bars were calculated as:

$$E_b = \frac{(T_{\max} - T_{\min})}{G} \quad E_{c1} = \frac{(T_{\max} - T_{\min})}{G} \quad E_{c2} = \frac{(T_{\max} - T_{\min})}{G} \qquad (5.4.3.)$$

where: E_b, E_{c1}, and E_{c2} are the error bars obtained for burial, slow cooling (in PAZ) and fast cooling. They were calculated considering the maximum and minimum paleotemperatures (T_{max} and T_{min}) obtained from modelling results in the inflection points for AFT and (U-Th)/He ages.

For three tectonic units, namely the Bucovinian, Tarcău and Subcarpathian nappes, two to three samples have been analysed. The values have been added together and the mean age per unit was further used for geological interpretation. In samples P7, P8 and P11, the computed burial and cooling amounts and rates represent the maximum estimations because no inverse thermal modelling could be performed, estimations are based on foreword modelling. Here, He closure temperature of 75°C was chosen as the maximum burial temperature experienced by the samples because He reset ages suggest that the rock samples have been buried at least above or close to this temperature, long enough to cause total diffusion of helium. Thermal models are present in Fig. 5.9a, with values in Table 5.2 and description in text.

5.5. Results and interpretations

The computed t-T paths of the SE Carpathian samples are based on the AFT and (U-Th)/He ages, spanning from Early Cretaceous to late Early Pleistocene. The results reveal exhumation and sometimes provenance ages; the former can be generally related to the orogenic events, while the latter give insights on the source areas. The previous published AFT data of Sanders et al. (1999) are also considered.

5.5.1. Bucovinian/Baraolt/Ceahlău nappes

The four samples collected from the post-tectonic conglomeratic cover of the Bucovinian nappe (O6, O7, O8 and O13; Fig. 5.3) revealed Albian AFT ages (103±11 and 101±12 Ma/O6 and O8) similar to stratigraphy/deposition and Aptian provenance ages (119-118±12 Ma/O7 and O13) (Fig. 5.4a). He ages are Lutetian (47±4 and 44±5 Ma/O7 and O8), Rupelian (29±3 Ma/O13) and Chattian (27±3 Ma/O6). Decomposing the age distribution for each sample resulted in two age groups: a minimum age that is slightly younger than the stratigraphy and an older age that was interpreted as provenance age (Table 5.1; Figs. 5.5 and 5.9c). Samples O6 and O13 reached maximum temperatures of 90 and 85°C, respectively, which indicate that the rocks entered and remained within the upper part of the PAZ. The samples did not reach temperatures high enough to totally anneal the fission-tracks.

The older decomposed AFT age group (provenance) ranges from Kimmeridgian to Hauterivian (152±53 to 134±15 Ma/O6, O7, O8, and O13; Fig. 5.9c and Table 5.1). These data together with the reset AFT age of 134 Ma located southward of the studied profile (Sanders et al, 1999; Fig. 5.3), indicate that the crystalline basement of the Bucovinian nappe was exhumed at that time and acted as a source area for the adjacent eastern

basin of the Subcarpathian nappe, as shown by its Kimmeridgian-Aptian provenance ages (136±14 and 72±7 Ma/P7 and P8; Fig. 5.3).

The Bucovinian basement underwent erosion until the Late Albian, when fast subsidence resumed, with deposition of unconformable continental conglomerates until the Cenomanian (O6, O13; Figs. 5.9a and 5.10). The corresponding rate was 0.3±0.04 mm/yr (Table 5.2). The nappe experienced again cooling at a very slow rate of 0.01±0.03 mm/yr during the Turnonian. An Upper Cretaceous-Eocene flysch package has been deposited on top of the nappe, these sediments have been subsequently partially removed, and presently, they occur only in the eastern part of the nappe. AFT minimum ages (O6 and O13; Fig. 5.8c) indicate that the nappe underwent cooling during the Santonian-Campanian, which is known as the "Laramian phase" in the Romanian literature (Fig. 5.12). Erosion affecting this nappe shed sediments to the eastern Subcarpathian (and Tarcău) basin as shown by the Campanian minimum provenance ages (80±10 Ma/P7 and 71±6 Ma/P6) and pooled age of 72±7 Ma in P8 (Figs. 5.3 and 5.8c). The cooling caused by erosion has continued until the Chattian (~28 Ma; Table 5.2) as seen by the flysch-like sediments presently found in the SW part of the Braşov basin and in the Homorod sub-basin (Fig. 5.3). The nappe cooled from Chatting to Dacian (~5 Ma) at a rate of 0.1±0.04 mm/yr (Table 5.2 and Fig. 5.10). The Chattian provenance age recorded eastward in the Pontian strata of the Focşani basin (27±5 Ma/P12; Figs. 5.3 and 5.8c) is coeval with onset of cooling in this nappe, making it a likely source area. The subsequent Dacian-Romanian subsidence and Quaternary cooling cannot be differentiated because of the insufficient resolution of the data (thermal models in Fig. 5.9a).

The evolution of the Baraolt nappe can be constrained with results from sample O1, which yield Campanian AFT (76±7 Ma) and Chattian He (23±3 Ma) ages (Figs. 5.3 and 5.8c). Because of inadequate inverse modelling result, a forward model was performed (Fig. 5.9a). The Baraolt nappe has been emplaced during the intra-Albian, when came in contact with the eastern Ceahlău nappe ("Austrian phase" in Romanian literature; Săndulescu et al., 1981). The subsequent subsidence indicated by the Upper Albian-Cenomanian post-tectonic sedimentary cover (Figs. 5.9a and 5.10) had a corresponding rate of 0.3 ±0.04 mm/yr (Table 5.2). The maximum burial temperature of ~85°C indicates that the rocks reached the middle part of the PAZ (Fig. 5.9a), from where they cooled slowly at a rate of 0.02±0.01 mm/yr (Table 5.2). The AFT cooling ages of 76±7 Ma (O1) and 72 Ma located south of the Braşov locality (Sanders et al., 1999; Fig. 5.3), indicate that the Baraolt nappe was affected by a second less intensive deformation during the Late Campanian, similar as in the Bucovinian nappe (Fig. 5.12). This period of deformation corresponds to the Late Campanian-Maastrichtian event ("Laramian phase").

Unroofing of this nappe provided a significant sedimentary input for the eastern subsiding Tarcău-Subcarpathian basin. The exhumation became faster around 23 Ma, Chattian (He age; Fig. 5.9a), reaching 0.1±0.09 mm/yr (Table 5.2). This rate of exhumation is comparable with that one recorded westward in the Bucovinian nappe. The Late Chattian provenance age recorded eastward in the Pontian strata of the Focşani basin (24±4 Ma/P13; Figs. 5.3 and 5.8c) indicates this nappe as the source area. The Pliocene subsidence and Quaternary cooling could not be separated.

In the Ceahlău nappe, Lutetian AFT and Chattian He ages (44±5 and 26±2 Ma/O3; Figs. 5.3 and 5.8c) have been obtained. Thermal history was derived from AFT and He

ages and forward modelling (Fig. 5.9a). Following the intra-Albian emplacement, the nappe experienced very fast burial during the Late Albian-Cenomanian (Figs. 5.9a and 5.10) up to 0.3±0.04 mm/yr (Table 5.2 and Fig. 5.10). During the Turonian-Chattian, the erosion-related cooling was similar as in the Bucovinian and Baraolt nappes (~27 Ma; Figs. 5.9a and 5.10), having a rate of ~0.02±0.02 mm/yr (Table 5.2 and Fig. 5.10). The sample reached a maximum burial temperature of 90°C, high enough to anneal almost completely the fission-tracks. The AFT and He ages indicate that exhumation was more accelerated during the Eocene.

AFT age population suggests that exhumation was already initiated during the Early Paleocene (63±6 Ma) and continued during the Eocene (36±6 Ma) and Oligocene (Fig. 5.12). The Paleocene-Eocene exhumation is confirmed by the similar provenance ages recorded further to the east, e.g. Paleocene in the Romanian strata of the Focşani basin (63 Ma/P18) and Eocene in the Subcarpathian nappe (55 Ma/P10; 50 Ma from Sanders et al., 1999), in the Sarmatian (50 Ma/P11) and Pontian strata (40 Ma/P12 and P13) of the Focşani basin (Fig. 5.3). The cooling continued from Chattian to Dacian (Figs. 5.9a and 5.10) at a rate of 0.1±0.07 mm/yr (Table 5.2 and Fig. 5.10). Since the Dacian, the subsidence and subsequent cooling caused by exhumation affected the area similarly to the more internal nappes (Fig. 5.10).

5.5.2. Tarcău/Marginal Folds/Subcarpathian nappes

The four samples collected from the Tarcău nappe (P25-P28, Fig. 5.3) yield Burdigalian-Badenian AFT ages (15±2, 12±1, 18±3 and 14±2 Ma/P25 to P28) and three of them displayed Badenian and Meotian He ages (12±1, 8±1 and 8±1 Ma/P25, P27 and P28; Fig. 5.3). The pre-Cretaceous to Middle Eocene subsidence and deposition have been followed by the Danian-Lutetian deposition of the dated sample. The modelling results show that the nappe underwent burial until the Early Burdigalian (~20 Ma; Figs. 5.9a and 5.10) at an average rate of 0.2±0.03 mm/yr (Table 5.2). The rock samples reached a temperature close to 105°C (P25 and P26; Fig. 5.9a), high enough to cause near total or total annealing of the fission-tracks. The onset of cooling can be placed in the Early Burdigalian, which continued until the Holocene (Fig. 5.12) at the rate of 0.2±0.03 mm/yr (Table 5.2 and Fig. 5.10). The eroded sediments were deposited in the eastern foreland basin, known as the Dacic basin since the Middle Miocene (Badenian). One can be noticed that the sample during cooling (Dacian-Romanian) was located at some depth.

Eastward in the Marginal Folds nappe, samples P20 and P4 have been analysed for AFT and (U-Th)/He methods (Figs. 5.3 and 5.8c). Unlike sample P4, the low-U content in apatites of sample P20 limited the number of enough fission-track measurements needed to carry out the AFT modelling. In contrast, sample P4 gave excellent results (Fig. 5.9a), with Sarmatian AFT (10±2 Ma) and late Early Pleistocene He (1±0) ages. Similar as in the Tarcău nappe, the results show that burial took place during the entire Cretaceous and continued until the Late Burdigalian (~18 Ma; Figs. 5.9a and 5.10) at a rate of 0.1±0.02 mm/yr (Table 5.2). A maximum burial temperature of ~115°C, close to the temperature of the total annealing of the fission-tracks, was reached. Modelling results of the bimodal length distribution show that the nappe remained within the PAZ from Late Burdigalian to Earliest Pleistocene (Figs. 5.9a and 5.10), cooling at a rate of 0.05±0.03 mm/yr (Table 5.2), with associated dominant fission-tracks of ~13-11 μm (Fig. 5.9b). Since the late Early

Figure 5.11

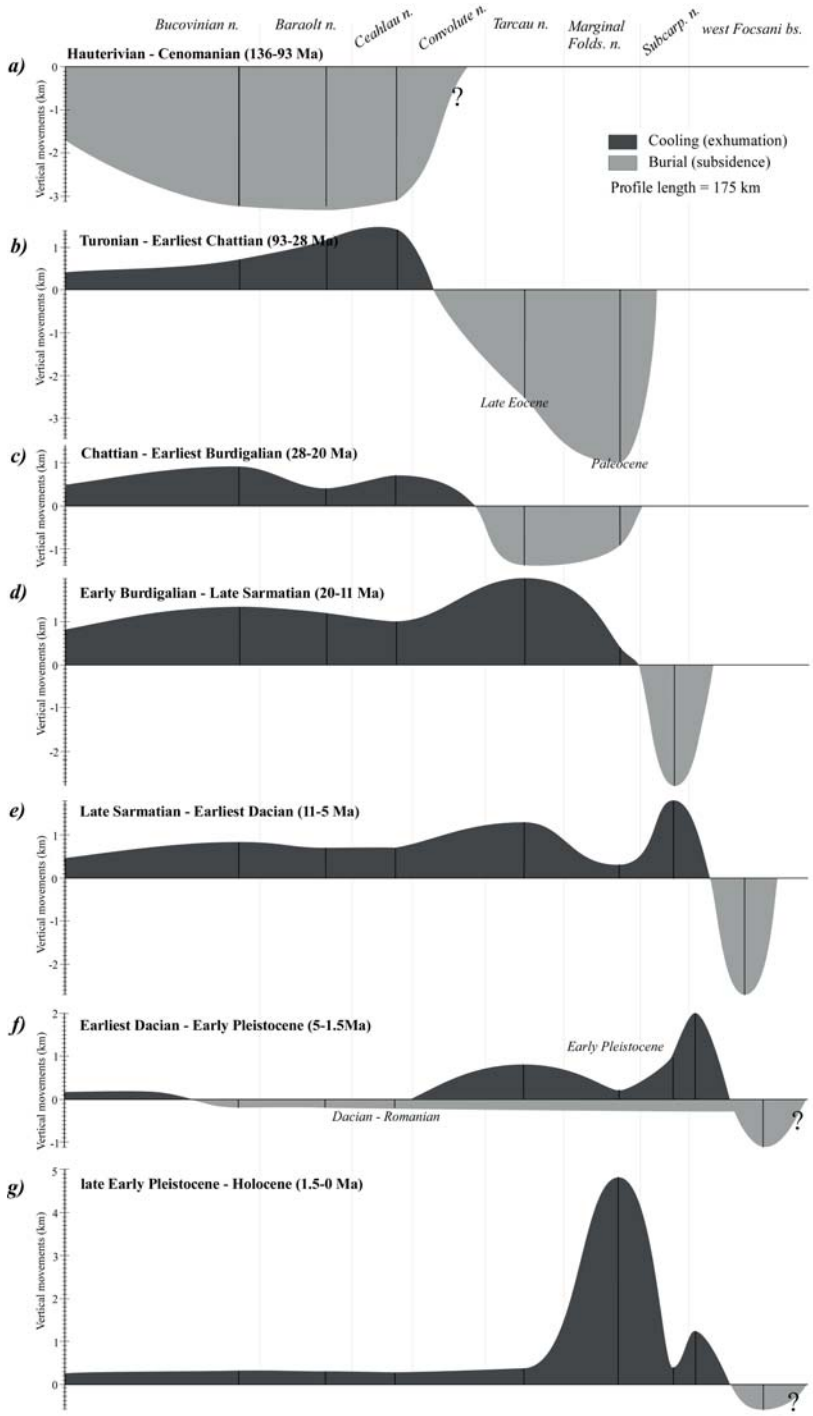

Amplitude of vertical movements recorded from Hauterivian/Albian to Holocene in the SE Carpathian orogen (a-g phases, discussion in text). Notice that the subsidence centre migrated eastward from Late Cretaceous to Quaternary, while the maximum exhumation was recorded in the Marginal Folds nappe during the Quaternary. Dark-grey colour stands for exhumation, while light-grey for burial.

Pleistocene (~1.5 Ma), the cooling became more accelerated and continued at this rate until the Holocene (Figs. 5.9a and 5.10). This is the highest recorded exhumation rate from all nappes, reaching 3.2±0.3 mm/yr (Table 5.2), with associated fission-tracks of 16-14 μm (Fig. 5.9b).

In the Subcarpathian nappe, the four samples analyzed yield reset (U-Th)/He ages, Badenian (15±2 Ma/P7 and 14±2 Ma/P9) and Meotian (7±1 Ma/P8, P10; Figs. 5.3 and 5.8c). The provenance AFT ages from this nappe reveal three age groups: Hauterivian (136±14 Ma/P7), Turonian (91±9 Ma/P6) and Campanian (72±7 Ma/P8, P10; Fig. 5.4a). After deposition during the Burdigalian, the rock samples experienced rapid burial reaching a temperature close to the He closure temperature (75°C), yet not resetting the AFT ages. The nappe underwent burial during the Badenian-Early Sarmatian (Figs. 5.9a and 5.10) at a rate of 0.9±0.03 mm/yr. This was followed by cooling due to exhumation until the present (0.3±0.06 mm/yr; Table 5.2). The source of the apatites with non-reset Hauterivian to Campanian AFT ages can be placed in the Bucovinian nappe, located in the western part of the study area.

5.5.3. Western flank of Focşani foreland basin

The five samples dated for the western flank of the Focşani basin (P11, P12, P13, P14 and P15; Fig. 5.3) have been collected from all stratigraphical units, except for the Quaternary. From old (W) to young (E), they comprise: Sarmatian, Pontian, Meotian, Dacian and Romanian strata (age limits from Vasiliev et al., 2004, 2005; values in Table 5.1). The ages obtained from AFT and (U-Th)/He analyses are much older than the stratigraphy, which indicate provenance ages. This does not apply to one, the He age from the Sarmatian strata (4±0 Ma/P11; Figs. 5.3 and 5.8a-b). The mean AFT provenance ages fall around Priabonian-Chattian (35±6 to 24±4 Ma/P18, P11-P14; Figs. 5.3 and 5.8a) and suggest as a source area the exhumed Bucovinian/Baraolt/Ceahlău nappes. The He ages range from Aquitanian (21±3 Ma/P11) to Meotian (10±1 and 9±1 Ma/P18, P13-P14; Figs. 5.3 and 5.8b), indicating source areas in the Tarcău nappe, and respectively, in the Marginal Folds and Subcarpathian nappes. The Sarmatian strata buried until the Late Dacian (4±0 Ma; Fig. 5.10) at a minimum rate of 0.4±0.06 mm/yr, were subsequently cooled until the present at ~0.8±0.1 mm/yr (Table 5.2).

5.6. Reconstructing the source to sink setting and regional tectonic implications

Low-temperature thermochronological dating across a profile in the SE Carpathian orogenic system yields ages spanning from late Early Cretaceous to late Early Pleistocene. This interval is coeval with the entire contractional evolution of the East Carpathians, from the Cretaceous oceanic subduction stage to the Miocene overthrusting of the European passive continental margin, and ultimately, docking of the orogenic system against the European and Moesian platforms. The relationship between the mountain chain providing material (source) and the depositional area (sink) is reconstructed both in time and space.

The Late Jurassic-Earliest Cretaceous age group from the Albian post-tectonic cover of the Bucovinian nappe (152±53 to 134±15 Ma/samples O6, O7, O8 and O13 in Fig. 5.9c

and 134 Ma age of Sanders et al., 1999 in Fig. 5.3) can be related to the erosion of the source areas along the passive margin of the Transylvanides ocean and to the opening and spreading of the eastern Ceahlău-Severin ocean. Situated between these domains, the Bucovinian system was likely affected by extensional related exhumation. The most likely source area is the Ceahlău-Severin domain because provenance ages are closer in time to the continental break-up, therefore, to a potential unroofing mechanism.

5.6.1. Hauterivian-Cenomanian (~136-93 Ma): emplacement of internal nappes and subsequent subsidence

The basement of the Bucovinian nappe experienced slow unroofing during the Hauterivian-Albian (Fig. 5.13a). This reflects the onset of the stacking of the internal Bucovinian nappe, which peaked during the intra-Albian (~105 Ma) phase of collision in the Transylvanides domain, and during thrusting over the Ceahlău-Severin sediments ("Austrian" phase; Săndulescu, 1988). Coeval subsidence took place eastward in the foreland of the advancing Bucovinian nappe, which progressively provided sedimentary input, in particular for the Subcarpathian basin (Fig. 5.13a). The previous deep oceanic sedimentation that took place in the depositional domain of the Baraolt/Ceahlău nappes, was gradually replaced up-sequence by turbidites, while finer sediments ("black shales") have been deposited in the more distal areas (Tarcău/Marginal Folds nappes) further to the east (Fig. 5.13a).

The burial-exhumation curves of the Bucovinian/Baraolt/Ceahlău nappes show that subsidence took place during the Late Albian-Cenomanian (Fig. 5.12). The thick conglomerates deposited over the intra-Albian nappe contacts (e.g. Bucegi conglomerates; Fig. 5.13a) have been laterally replaced by finer sediments in the Convolute nappe (sandstones) and Tarcău/Marginal Folds nappes (mudstones), reflecting a similar sedimentary source and paleobathimetric configuration.

The maximum temperatures of 90/90/85°C reached by the post-tectonic covers of the Bucovinian/Baraolt/Ceahlău nappes (Fig. 5.9a) indicate comparable burial depths (~3 km). Under these conditions, the AFT ages and mean size of etch-pits point to variable annealing conditions, i.e. partial annealing for the Bucovinian cover and total annealing for the Baraolt and Ceahlău nappes. The differential annealing might be explained by the variable annealing kinetics of the studied apatites, which are more retentive for fission-tracks (Cl-rich) in the Bucovinian nappe (1.7-2.0 μm), more sensitive to annealing in the Ceahlău nappe (1.6 μm) and not very clear for the Baraolt nappe (2.0 μm).

5.6.2. Turonian-Earliest Chattian (93-28 Ma): slow exhumation in the internal nappes and subsequent subsidence in the east

The internal deformation of the Bucovinian/Baraolt/Ceahlău nappes and their eastward thrusting over the external units during the Late Campanian-Maastrichtian "Laramian" phase (~75-68 Ma) is shown by the (Santonian) Campanian exhumation of the Bucovinian cover (samples O6-O8, O13) and Baraolt nappe (O1) and by the Campanian provenance ages of the Subcarpathian nappe (samples P6-P8; Figs. 5.3 and 5.9c). The Ceahlău nappe underwent slightly younger exhumation, which started in the Paleocene (sample O3, Figs. 5.3 and 5.9c). This nappe became source area for the Subcarpathian basin (sample P11 and Sanders et al., 1999), from where the sediments have been subsequently eroded and re-deposited as the Sarmatian/Pontian/Romanian strata in the

Focşani basin (Fig. 5.3). The nappes exhumation indicates that the shortening became younger eastward and was continuous from Late Cretaceous to Paleogene, resulting in reduced amounts of exhumation (Figs. 5.11b and 5.13b).

All these observations are compatible with the model of an accretionary wedge active during the Late Cretaceous-Paleogene, the sediments being scraped-off from the gradually subducting Ceahlău-Severin ocean. The cooling continued slowly in all three internal

Figure 5.12

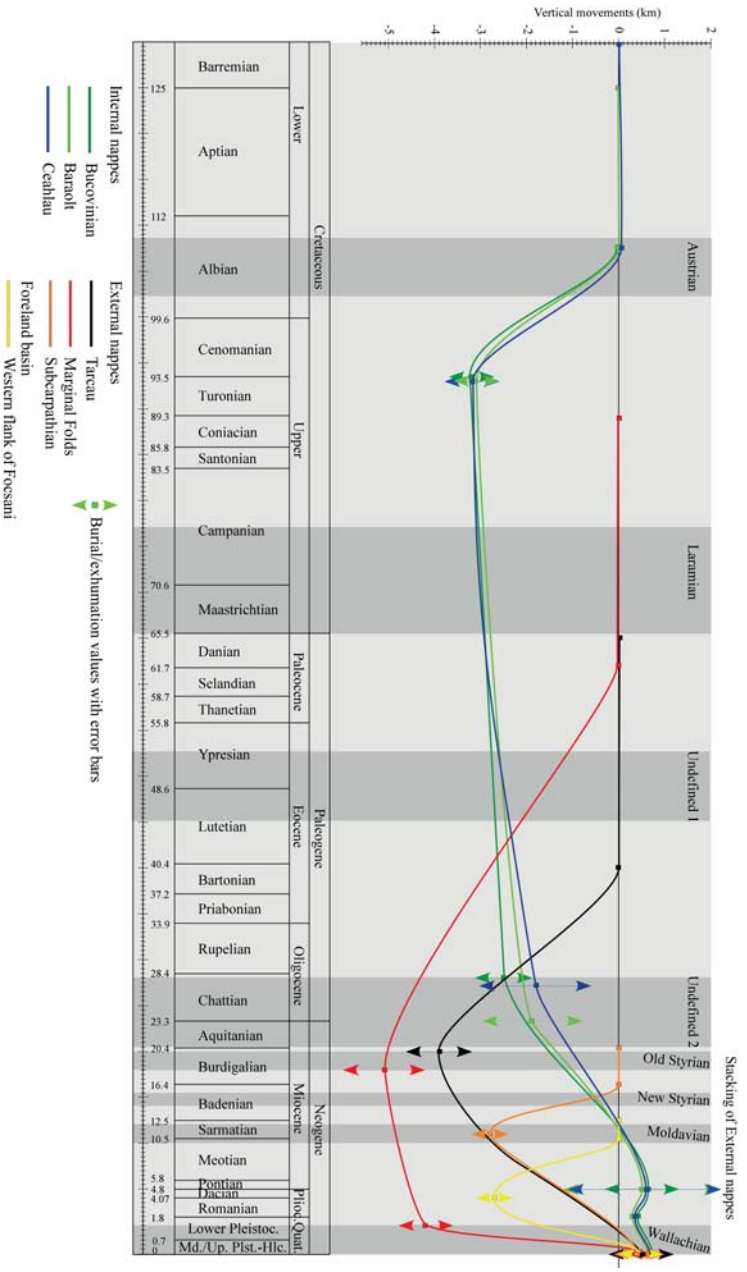

Burial-cumulative exhumation curves vs. time for the SE Carpathian nappes. The different colours stand for: dark-green/light-green/blue for the internal Bucovinian/Baraolt/Ceahlău nappes; black/red/orange for the external Tarcău/Marginal Folds/Subcarpathian nappes; and yellow for the western flank of the Focşani basin. Squares from each slope represent the inflection points where tectonic regime changes. Notice that the time scale changes at 1.8 Ma for a better representation of the events during the Quaternary.

Figure 5.13

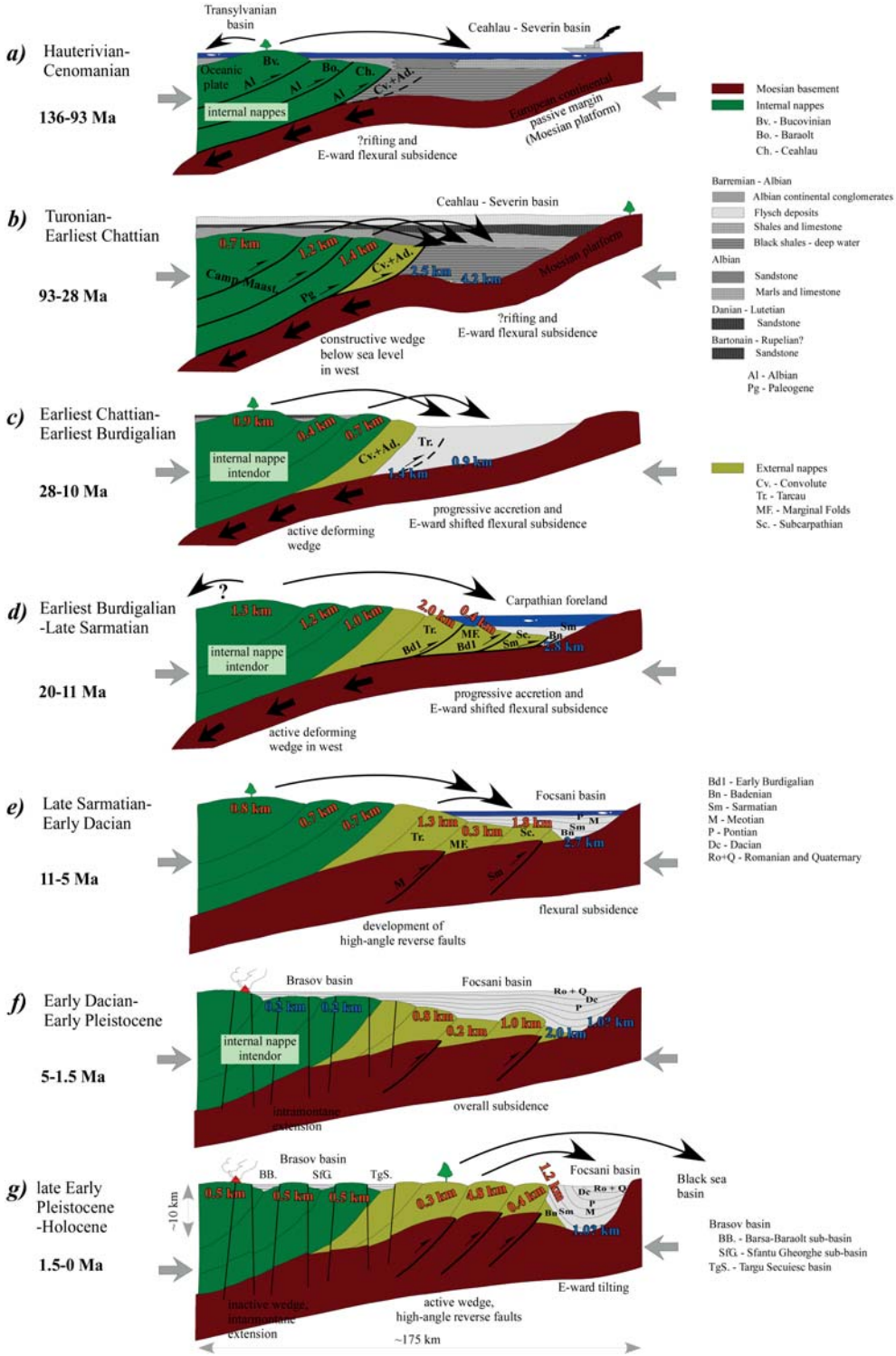
a) Hauterivian-Cenomanian
136-93 Ma
Transylvanian basin
Ceahlau - Severin basin
Oceanic plate
Bv.
Bo.
Ch.
Al
Cv.+Ad.
internal nappes
European continental passive margin (Moesian platform)
?rifting and E-ward flexural subsidence
b) Turonian-Earliest Chattian
93-28 Ma
Ceahlau - Severin basin
0.7 km
1.2 km
1.4 km
Cv.+Ad.
Camp-Maast.
Pg
4.5 km
4.2 km
Moesian platform
?rifting and E-ward flexural subsidence
constructive wedge below sea level in west
c) Earliest Chattian-Earliest Burdigalian
28-10 Ma
0.9 km
0.4 km
0.7 km
Cv.+Ad.
Tr.
0.9 km
1.4 km
internal nappe intendor
progressive accretion and E-ward shifted flexural subsidence
active deforming wedge
d) Earliest Burdigalian -Late Sarmatian
20-11 Ma
?
Carpathian foreland
1.3 km
1.2 km
1.0 km
2.0 km
0.4 km
Tr.
MF.
Bd1
Sc.
Sm
Bn
2.3 km
internal nappe intendor
progressive accretion and E-ward shifted flexural subsidence
active deforming wedge in west
e) Late Sarmatian-Early Dacian
11-5 Ma
Focsani basin
0.8 km
0.7 km
0.5 km
1.3 km
0.3 km
1.8 km
Tr.
MF.
Sc.
Bn
Sm
M
P
2.7 km
flexural subsidence
development of high-angle reverse faults
f) Early Dacian-Early Pleistocene
5-1.5 Ma
Brasov basin
Focsani basin
0.3 km
0.3 km
0.8 km
0.2 km
1.0 km
2.0 km
Ro + Q
Dc
P
1.0 km
internal nappe intendor
overall subsidence
intramontane extension
g) late Early Pleistocene -Holocene
1.5-0 Ma
~10 km
Brasov basin
BB.
SfG.
TgS.
Focsani basin
Black sea basin
0.5 km
0.5 km
0.6 km
0.3 km
0.3 km
0.4 km
1.2 km
Dc
Ro + Q
P
M
Bn
Sm
1.02 km
E-ward tilting
inactive wedge, intramontane extension
active wedge, high-angle reverse faults
~175 km
Moesian basement
Internal nappes
Bv. - Bucovinian
Bo. - Baraolt
Ch. - Ceahlau
Barremian - Albian
Albian continental conglomerates
Flysch deposits
Shales and limestone
Black shales - deep water
Albian
Sandstone
Marls and limestone
Danian - Lutetian
Sandstone
Bartonain - Rupelian?
Sandstone
Al - Albian
Pg - Paleogene
External nappes
Cv. - Convolute
Tr. - Tarcau
MF. - Marginal Folds
Sc. - Subcarpathian
Bd1 - Early Burdigalian
Bn - Badenian
Sm - Sarmatian
M - Meotian
P - Pontian
Dc - Dacian
Ro+Q - Romanian and Quaternary
Brasov basin
BB. - Barsa-Baraolt sub-basin
SfG. - Sfantu Gheorghe sub-basin
TgS. - Targu Secuiesc basin

nappes until the Earliest Oligocene, probably due to reduced contraction recorded during this period (Figs. 5.12 and 5.13b).

The nappes remained below the sea level during the Latest Cretaceous-Paleogene, resulting in the unconformable Eocene-Oligocene marine sedimentation on top of the internal Bucovinian nappe. This can be seen west of Braşov in the Vlădeni corridor (Săndulescu, 1972; Fig. 5.2) or in the Maastrichtian-Paleogene sediments overlying the frontal part of the Ceahlău nappe (Melinte and Jipa, 2005). Local faster subsidence was recorded in the Marginal Folds basin since the Paleocene, where reached a maximum of 4.2 km. Progressively, it extended westward and covered the Tarcău basin during the Late Eocene (Fig. 5.11b), the subsidence centre roughly overlapping the Subcarpathian basin (Figs. 5.11b and 5.13b). This can be interpreted as an effect of the regional relaxation after the Transylvanides collision and probably doubled by the flexural subsidence over the subducting Ceahlău-Severin ocean (Fig. 5.13b). Coeval to subsidence, the cooling continued in the internal nappes (Fig. 5.12) with the corresponding unroofing amount increasing from west to east, which indicates faster deformation in the Ceahlău nappe (Fig. 5.11b). The flysch deposition during the Late Cretaceous-Oligocene on top of the internal nappes and in the eastern foreland basin (Tarcău/Marginal Folds), has resulted in a thick package of sandstone with a maximum thickness of 3000 m in the Tarcău nappe (Fig. 5.13b), thinning towards the west (Săndulescu et al., 1981).

5.6.3. Early Chattian-Early Burdigalian (28-20 Ma): gradual exhumation of internal nappes and on-going subsidence in the foreland

Since the Late Oligocene, the internal nappes have been exhumed (Figs. 5.12 and 5.13c) with slightly different magnitudes. The cooling rate reached its maximum in the Bucovinian nappe, slowly decreasing in the Baraolt nappe and increased again eastward in the Ceahlău nappe (Table 5.2). As a result, a large part of the Cretaceous-Lower Oligocene overburden has been removed, with estimated values of 0.9±0.2, 0.4±0.5 and 0.7±0.5 km (Fig. 5.11c). Small sedimentary remnants are still preserved on top of these nappes, presently occurring in the Vlădeni basin (Figs. 5.3 and 5.13c). To the east, the subsidence reached a maximum of 1.4 km in the front of the Ceahlău thrust with depocentre in the Tarcău basin. The subsidence amplitude decreased by half to the east in the Marginal Folds basin (Fig. 5.11c).

The Late Oligocene differential exhumation can be interpreted as a renewed convergence between the internal nappes and the Moesian continental passive margin. The change from stability and subsidence to exhumation is possibly due to the arrival of the stretched continental part of the Moesian platform at the subduction zone (Fig. 5.13c). The renewed convergence might be trigged by the counterclockwise rotation and northward indentation of the Adria (Apulia) microplate, an appendage of Africa (Pinter et al., 2005), which induced large scale clockwise rotation of the Tisza-Dacia block around the Moesian platform (senso Raschbacher et al., 1993). The diachronous collision of Adria

◀ Figure 5.13
Tectonic evolution of the SE Carpathian orogen from Hauterivian/Albian to Holocene is divided into seven tectonic phases. The source to sink reconstruction is also presented (description in text). This figure is mainly restricted to sediments and shows the progressive growth of an accretionary wedge from Hauterivian/Albian to Late Sarmatian (dark- and light-green colours). It also shows high-angle reverse faults that affected the lower Moesian basement (brown colour) during the last orogenic phases, i.e. from Late Sarmatian to Holocene. Red values correspond to exhumation amount that was recorded by each nappe, while light-blue values indicate subsidence amount experienced by each nappe and Focşani basin. Notice that the horizontal and vertical scales refer to the present-day scenario.

with the European plate induced compression in the Alps, the Apennines, the Dinaride-Albanide-Hellenide mountain belt and the Carpathians-Pannonian region during the Late Oligocene-Early Miocene (Jolivet and Faccenna, 2000; Dilek, 2006; Schmid et al., 2008).

The Late Oligocene-Early Miocene exhumation of the internal nappes (this study; Bojar et al., 1998; Fügenschuh and Schmid, 2005; Schmid et al., 2008) led eventually to the gradual separation of the Transylvanian basin from the foreland in the SE Carpathian area, the accommodation space being shifted and limited west- and eastward, respectively. At a larger scale, this moment corresponds to the separation of the Central Paratethys (Pannonian and Transylvanian basins) from the Eastern branch (Carpathian basin, Black Sea up to the South Caspian Sea) due to the active mountain building processes taking place in the Alps-Carpathians-Taurides-Caucasus domain (Rögl, 1999). Back to the study area, unroofing of the newly formed topography in the internal Carpathian nappes provided coarse clastic sedimentary input for the adjacent basins, as recorded by the Priabonian-Rupelian AFT provenance ages in the Uppermost Miocene-Pliocene sedimentary sequence of the Focşani basin.

5.6.4. Early Burdigalian-Late Sarmatian (20-11 Ma): emplacement of external units and exhumation

Exhumation of the internal Carpathian nappes continued during the Miocene (Figs. 5.12 and 5.13d), reached a maximum amplitude of 1.3 km in the Bucovinian nappe (Fig. 5.11d). During the Early Burdigalian (~20 Ma), the deeper Paleogene coarse deposits accumulated at the toe of the Ceahlău thrust, continued to be accreted and subsequently exhumed due to the continuous convergence and westward subduction of the continental parts of the Moesian platform underneath of the locked internal nappes indentor (Fig. 5.13d). As a result, the exhumation affected areas as far east as the internal parts of the Tarcău nappe (Fig. 5.12). The present-day erosional contour of the Tarcău nappe in the study area displays only its internal parts, the external parts being subsequently removed by erosion. It can be studied north and south of the Vrancea half-window (Fig. 5.3), where the final stage of the thrusting took place in the intra-Badenian. The Early Burdigalian event affected to a minor extent the depositional area of the Marginal Folds nappe, the nappe remaining within the temperature range of the PAZ until the Early Pleistocene (Figs. 5.12 and 5.13d). One can be concluded that the exhuming event covered larger areas than previously assumed over the Audia/Convolute/Macla nappes (Săndulescu, 1988; Gibson, 2001). The subsequent flexural subsidence recorded in the most external Subcarpathian nappe (Figs. 5.12 and 5.13d), was coeval with the onset of the back-arc subsidence in the Transylvanian basin (Krézsek and Bally, 2006). In the depositional area of the Subcarpathian nappe, subsidence reached 2.8±0.4 km (Fig. 5.11d) until the Sarmatian, which corresponds to the onset of exhumation. During the Early Burdigalian-Late Sarmatian, the subsidence depocentre was progressively shifted eastward and was compatible with the flexural subsidence related to a gradual emplacement of the nappes towards the eastern foreland basin.

5.6.5. Late Sarmatian-Early Dacian (11-5 Ma): collision, post-collisional exhumation and foreland subsidence

The Miocene contractional phase that peaked in the Sarmatian (~11 Ma) is shown by the clustering of the exhumation and provenance ages. The subsequent period was

characterised by asymmetric and out-of-sequence exhumation recorded in the external orogenic nappes (Fig. 5.13e). In the internal units, the exhumation pattern remained unchanged. Significant change took place in the external Tarcău/Marginal Folds/Subcarpathian nappes (Figs. 5.11e, 5.12 and 5.13e). The flexural loading space created by the thrusting of the Subcarpathian nappe over the foreland shifted once again the depocentre to the east. It resulted in formation of the Focşani foredeep, which overlapped the previous Badenian subsidence (Tărăpoancă et al., 2003). This basin was filled with clastic sediments (Fig. 5.13e). The asymmetric subsequent exhumation of the Tarcău nappe since the Early Burdigalian and of the Subcarpathian nappe since the Late Sarmatian (Fig. 5.12) can be related to high-angle reverse faults which truncated the lower Moesian basement during the last orogenic phases (Roure et al., 1993). These foreland-coupling events have been previously associated with a Quaternary post-collisional out-of-sequence renewed contraction in the SE Carpathians (Matenco et al., 2007). The asymmetric exhumation derived during this study points to the possibility that the assumed Quaternary contractional event started earlier during the Latest Miocene. It could be responsible for removal of 1.3±0.3 and 2.3±0.3 km of overburden from the Tarcău and Subcarpathian nappes, respectively, (Fig. 5.12). The Marginal Folds nappe remained rather stable during this time (Figs. 5.11e and 5.13e). These contractional events can be correlated with the erosion exposure of the entire Transylvanian basin during the Late Pannonian (Krézsek and Bally, 2006), which in the Eastern Paratethys timescale is equivalent to the Late Meotian (Vasliev et al., 2004). The Sarmatian-Meotian provenance He ages obtained from the Pliocene strata of the Focşani basin are comparable with the exhumation of the Tarcău and Subcarpathian nappes, making them likely source areas. However, during the entire period, subsidence and deposition continued within the Focşani basin (Fig. 5.12), accumulating more than 7 km of sediments (Tărăpoancă et al., 2003).

5.6.6. Early Dacian-Early Pleistocene (5-1.5 Ma): overall subsidence and subsequent eastward exhumation

Since the Pontian, extension affected the internal part of the orogen resulting in formation of the Braşov intramontane basin (Fig. 5.13f), the associated deep-rooted normal faults proving pathways for the alkaline volcanism to the surface (Girbacea and Frisch, 1998; Fielitz and Seghedi, 2005; Seghedi et al., 2005).

During the Dacian-Romanian, palinspastic reconstructions have suggested that subsidence affected both the internal (not Bucovinian) and external nappes, and an open water connection existed between the Focşani and Braşov basins (Leever et al., 2006). Probably, the sediments were commonly deposited in the intramontane basin, on top of the external nappes and in the Focşani foreland. Presently, these sediments cannot be found on top of the external nappes, which allow to assume that either they were entirely removed by the Quaternary erosion or they were not deposited there. The water connection between the two basins could be done either along a narrow corridor or over a larger lake.

Thermal modelling results suggest that the Tarcău and Subcarpathian nappes experienced continuous cooling due to the earlier described high-angle reverse faults (Fig. 5.13f), reaching a maximum of 1 km in the Subcarpathian nappe (Fig. 5.11f). Coeval, the Marginal Folds nappe still remained at a few kilometres deep in the temperature range of the PAZ (Figs. 5.12 and 5.13f). The exhumation probably kept pace with deposition in most of the areas outside the peak measured exhumation (Fig. 12f), while the water

connection was still ensured between the Braşov basin and the foreland. The connection was probably along a narrow corridor, i.e. Buzău valley, than over a larger lake. The Buzău river flowed initially northward into the Braşov basin and changed its course during the Quaternary to the SE towards the Focşani basin (Rădoane et a., 2003), probably due to the exhumation of the external nappes (AFT data; Merten et al., 2006, Sanders et al., 1999). Since the Romanian, the Sarmatian strata from the Focşani basin experienced exhumation of 2.0±0.3 km (Figs. 5.11f and 5.13f), which extended westward in the internal nappes during the Early Pleistocene.

From the above data can be concluded that contraction affected continuously the external nappes and the western flank of the Focşani basin (Fig. 5.13f), coeval with extension in the internal part of the orogen, i.e. Braşov basin (Girbacea and Frisch, 1998; Fielitz and Seghedi, 2005; Seghedi et al., 2005). Several mechanical models have been proposed over time to explain post-orogenic extension and contraction in convergent orogens (see a compilation in Willett, 1999). In the SE Carpathians, partial delamination of continental mantle lithosphere (Chalot-Prat and Gîrbacea, 2000), slab-driven such as slab-pull and/or roll-back of the Carpathians embayment (Royden, 1993) etc. have been proposed.

5.6.7. Late Early Pleistocene-Holocene (1.5-0 Ma): overall exhumation

The exhumation did not exceed more than few hundreds of meters in the area comprised between the internal Bucovinian and the external Tarcău nappes. It increased to 0.6±0.1 km in the Subcarpathian nappe and to 1.2±0.2 km on the western flank of the Focşani basin (Fig. 5.11g). These amounts are significantly smaller than that one recorded in the Marginal Folds nappe since the late Early Pleistocene (Figs. 5.11g and 5.13g). Here, the exposure of the Lower Cretaceous sediments in the centre of the Vrancea half-window requires removal of 4.8±0.4 km of overburden (Figs. 5.11g and 5.12) and must be connected with the previously described high-angle reverse faults affecting the Moesian basement. Unroofing of the Marginal Folds nappe might be responsible for the 9°ENE-ward tilting of the Lowermost Pleistocene strata from the foreland basin (Necea et al., 2005). This compressional phase was previously described as the Wallachian phase, SW of the study area along the Buzău valley (Hippolyte and Săndulescu, 1996). At present, the sedimentary deposits from the Focşani basin are strongly tilted eastward, with dip reaching 87° for the Sarmatian and decreasing to 15° for the Romanian strata (Fig. 5.13g). The strong tilting of these strata might be a consequence of the continuous unroofing affecting the orogen coupled with subsidence in the basin centre.

5.7. Conclusions

The kinematics of the SE Carpathian orogenic system was revised based on the new AFT and (U-Th)/He data coupled with the previous published literature. The results show that after the Late Jurassic-Earliest Cretaceous oceanic spreading in the Transylvanides and Ceahlău-Severin domains, a period of continuous shortening took place from late Early Cretaceous to Present as seen by the eastward-foreland-vergent thrusting. Two major kinematic intervals have been distinguished: (1) late Early Cretaceous to Late Miocene progressive evolution of an accretionary wedge and (2) Latest Miocene to Present post-collisional high-angle reverse faulting.

(1). Late Early Cretaceous-Late Miocene accretionary wedge. Stacking of the internal nappes during the late Early Cretaceous, with a peak deformation in the intra-Albian

(Austrian phase) was due to collision in the Transylvanides domain. Subsequent Late Albian-Cenomanian rapid subsidence followed in the internal nappes. During the Late Cretaceous-Paleogene, shortening affecting these nappes and their sedimentary covers was continuous, but reduced in amplitude. The nappes remained below the sea level, but probably providing sedimentary input for the eastern subsiding Tarcău and Subcarpathian areas. The internal nappe contacts were covered by an unconformable Upper Cretaceous-Paleogene flysch sequence with variable thicknesses. The subsidence took place after the Transylvanides collision and superposed the flexural subsidence over the subducting Ceahlău-Severin domain. Exhumation affecting the internal nappes since the Late Oligocene is due to the renewed convergence between the internal nappe indentor and the Moesian continental passive margin, trigged by the clockwise rotation of the Tisza-Dacia block around the Moesian platform. It resulted in the gradual separation of the Transylvanian basin from the foreland, the internal nappes sourcing material to both basins. The Miocene corresponds to the gradual emplacement of the external nappes as a result of continuous advancing and westward subduction of the Moesian platform underneath of the internal nappe indentor. The depocentre of the flexural subsidence was shifted eastward due to the progressive nappe emplacement towards the foreland basin. The external nappe stacking ended during the Late Miocene, when they came in direct contact with the Moesian platform.

(2). Latest Miocene-Present post-collisional high-angle reverse faulting. The post-Late Miocene exhumation of the external nappes was due to the post-collisional renewed shortening, the nappes progressively providing material for the Uppermost Miocene-Pliocene sequence of the Focşani basin. The exhumation extended westward during the Late Pannonian (Meotian) and reached the Transylvanian basin. Since the Latest Miocene (Pontian), the internal nappes underwent extension, resulting in formation of the Braşov basin, which was probably connected with the Focşani basin. The connection between the two basins was probably done rather along a narrow corridor, i.e. Buzău valley, than over a larger lake. During the Late Pliocene, the Sarmatian strata of the Focşani basin have been affected by exhumation, which extended during the Early Pleistocene as far west as the internal nappes. In the late Early Pleistocene, it covered slowly the most-external nappes and the western flank of the Focşani basin. The coeval exhumation recorded in the central external nappe is due to the same reverse fault system, which resulted in tilting of the Lowermost Pleistocene strata.